

Modeling, Analysis & Mitigation of VFTO in GIS

Major Project Report

Submitted in Partial Fulfillment of the Requirements

For the degree of

Master of Technology

In

Electrical Engineering

(Power Electronics, Machines and Drives)

By

Meet J Patel

14MEEP20



DEPARTMENT OF ELECTRICAL ENGINEERING

INSTITUTE OF TECHNOLOGY

NIRMA UNIVERSITY

AHMEDABAD-382481

MAY 2016

Undertaking for Originality of the Work

I **Meet Patel**, Roll No. **14MEEP20**, give undertaking that the Major Project entitled **Modeling, Analysis & Mitigation of VFTO in GIS** submitted by me, towards the partial fulfilment of the requirements for the degree of Master of Technology in **Power Electronics, Machines and Drives**, of Institute of Technology, Nirma University, Ahmedabad, is the original work carried out by me and I give assurance that no attempt of plagiarism has been made. I understand that in the event of any similarity found subsequently with any published work or any dissertation work elsewhere, it will in severe disciplinary action.

Signature of student

Date:

Place: Ahmedabad

Endorsed by:

Industry Guide

Ms. Shefali K. Talati

Deputy Manager

TM-4 Power System

Research and Development

ERDA

Vadodara

Institute Guide

Prof. Chintan R. Mehta

Assistant Professor

Department of Electrical Engineering

Institute of Technology

Nirma University

Ahmedabad

Certificate

This is to certify that the Major Project Report entitled **Modeling, Analysis & Mitigation of VFTO in GIS** submitted by Mr. **Meet J. Patel**, Roll No. **14MEEP20**, towards the partial fulfillment of the requirements for the degree of Master of Technology (Electrical Engineering) in the field of Power Electronics, Machines & Drives of Nirma University is the record of work carried out by him under our supervision and guidance. The work submitted has in our opinion reached a level required for being accepted for examination. The results embodied in this major project work to the best of our knowledge have not been submitted to any other University or Institution for award of any degree or diploma.

Date:

Industry Guide

Ms. Shefali K. Talati

Deputy Manager

TM-4 Power System

Research and Development

ERDA

Vadodara

Institute Guide

Prof. Chintan R. Mehta

Assistant Professor

Department of Electrical Engineering

Institute of Technology

Nirma University

Ahmedabad

Head of the Department

Department of Electrical Engineering

Institute of Technology

Nirma University

Ahmedabad

Director

Institute of Technology

Nirma University

Ahmedabad

Acknowledgement

With immense pleasure, I would like to present this report on the dissertation work related to **Modeling, Analysis & Mitigation of VFTO in GIS**. I am very thankful to all those who helped me for the successful completion of the first phase of the dissertation and for providing valuable guidance throughout the project work.

I would first of all like to offer thanks to **Ms. Sefali K. Talati(Deputy Manager,Power System),ERDA,Vadodara** Project Guide whose interest and excellent knowledge base helped me to finalize the topic of the dissertation work. Her constant support, encouragement, and constructive criticism has been invaluable assets through my project work. She has shown interest in this dissertation work right from beginning and has been a great motivating factor in outlining the flow of my work.

I am also thankful to **Dr. M. K. Shah(Director),ERDA,Vadodara** for giving me a good opportunity to work in esteemed organization.

I am very much obliged to **Prof. Chintan R. Mehta(Asst.Professor, Electrical Engineering Department, Institue of Technology, Nirma University)** for his kind help and encouragement in my project work.

My sincere thanks **Prof Dr.P.N.Tekwani(Head of Electrical Engineering Department,Nirma University)** and **Prof.T.H.Panchal(Asst.Professor, Electrical Engineering Department, Institue of Technology, Nirma University)** for allowing me to do my project work at ERDA,Vadodara.I am thankful to Nirma University for providing all kind of required resources.

Finally, I would like to thank The Almighty, my family members for supporting and encouraging me in all possible ways. I would also like to thank my friends who have provided continuous encouragement in making this dissertation work successful.

- Meet J.Patel

Abstract

The increase in demand for electricity and the growing energy density in urban area have made it necessary to extend the existing high voltage network right up to the consumer. For these, Gas Insulated substation has been developed which consume minimum space, flexibility from environmental influences, high reliability, minimum maintenance, flexible operation and for future development to meet the present day requirements.

The power system should be reliable. One of the major reason of power system interruption is due to insulation failure because of ver fast transient over voltages in the power system. These overvaoltages has very steep rate of rise time. VFTO phenomenon is greatly affected in gas insulated substation and this effect is observed at most of the components in gas insulated substation. The major source of VFTO is operation of disconnecter switch or isolator. The main objective of this project is to perform modeling and simulation of VFTO in Gas Insulated Substation as well as analysis of VFTO across different equipments and to propose its mitigation techniques and compare the different techniques. Gas Insulated Substation has been modeled and simulated using EMTP-RV.

Abbreviations

VFTO	Very Fast Transient Overvoltage
GIS	Gas Insulated Substation
SF_6	Sulfur Hexafluoride
N_2	Nitrogen
GWP	Global Warming Potential
TEV	Transient Enclosure Voltage
TCV	Trapped Charge Voltage
TEMF	Transient Electromagnetic Field
EMTP	Electro Magnetic Transient Program
DS	Disconnect Switch
TGPR	Transient Ground Potential Rises
XLPE	Cross Linked Polyethylene
LIWV	Lightning Impulse Withstand Voltage

Nomenclature

μ	Magnetic permeability
ϵ_o	Permittivity Constant
ϵ_r	Relative Permittivity of Medium
K_c	Co-ordination Factor
K_s	Safety Factor
K_{tc}	Test Conversion Factor

Objective of the Project

Very Fast Transient Overvoltage is major problem in Gas Insulated Substation. The main objective of this project is to perform modeling and simulation of VFTO in Gas Insulated Substation. The analysis of VFTO across different equipments is performed and its mitigation techniques have been suggested and compare the different techniques. The guidelines to be followed by VFTO analysis are :

- CIGRE 519
- IEC 60071-4

Scope of the work

After completion of this work one can be able to know the generated VFTO in GIS across the connected equipments. This VFTO may lead to stress on the insulation to the connected equipments and by mitigating this VFTO, one can able to reduce the failure of equipment and increase the life of the equipment. By reducing VFTO, effectiveness and reliability of power system is increase.

Contents

Acknowledgement	iv
Abstract	v
Abbreviations	vi
Nomenclature	vii
List of Figures	xii
List of Tables	1
1 Introduction to Gas Insulated Substation	2
1.1 Introduction	2
1.2 Advantages of GIS	4
1.3 Disdvantages of GIS	5
2 Literature Review	6
2.1 Literature Review	6
3 Very Fast Transient Overvoltage	8
3.1 Where VFTO Occurs?	8
3.2 Origin of VFTO	8
3.3 How VFTO generated?	9
3.4 Characteristics of VFTO	9
3.5 Classification of VFTO	10
3.5.1 Internal transients	11
3.5.2 External transients	11
3.6 General VFTO Calculation Approach	12
3.6.1 Step1: VFTO Calculation	12
3.6.2 Step2: Required VFTO withstand level - Comparison with LIWV	13
3.6.3 Step3: Measures according to the insulation co-ordination . .	13
3.7 Operating voltage of GIS	14
3.8 Trapped Charges	15
3.9 Maximum VFTO stresses	15

4	Mitigation techniques for VFTO	16
4.1	VFTO suppression using damping resistor	16
4.2	VFTO suppression using hybrid compensation	17
4.2.1	L type compensation	18
4.2.2	T type compensation	18
4.3	VFTO suppression using ferrite ring	19
5	Calculation and Modeling of GIS Components	23
5.1	Single Line Diagram of GIS	23
5.2	Calculation of Various Parameters	24
5.2.1	Calculation of Transmission Line	24
5.2.2	Calculation of GIS Busbar	26
5.2.3	Calculation of XLPE cable	27
5.3	Modeling of Various components	29
5.3.1	Overhead Transmission Line	29
5.3.2	GIS Bushbar	30
5.3.3	XLPE cable	31
5.3.4	Circuit Breaker	32
5.3.5	Disconnecter Switch	33
5.3.6	Earthing Switch	33
5.3.7	Current Transformer and Potential Transformer	34
5.3.8	Bushing	34
5.3.9	Surge Arrester	35
5.3.10	Elbow	35
6	Simulation of GIS in EMTP-RV	36
6.1	Introduction to EMTP-RV	36
6.2	Types of simulation in EMTP-RV	37
6.3	Applications of EMTP-RV	37
6.4	Modeling of 400 kV single line diagram	38
6.5	Modeling of 400 kV GIS system with Damping Resistor	41
6.6	Effect of hybrid compensation on VFTO	44
6.6.1	Modeling of 400 kV GIS system with L type compensation . .	44
6.6.2	Modeling of 400 kV GIS system with T type compensation . .	47
6.7	Modeling of 400 kV GIS System with ferrite ring	51
6.8	Comparison of mitigation methods	54
7	Conclusion and Future scope	55
7.1	Conclusion	55
7.2	Future Scope	57
	References	58

List of Figures

1.1	Gas Insulated Substation	3
3.1	Characteristics of VFTO	10
3.2	Classification of VFTO	10
4.1	VFTO in relation to the resistance of the damping resistor	17
4.2	L type compensation	18
4.3	T type compensation	18
4.4	Cross section of ferrite ring	20
4.5	frequency and magnetic hysteresis coefficient scale of Mn-Zn ferrite	22
5.1	Single line Diagram of GIS System	23
5.2	Bundle conductor line	24
5.3	Inner conductor and outer enclosure of GIS	26
5.4	Cross section of XLPE cable	27
5.5	Transmission Line	29
5.6	GIS Busbar	30
5.7	XLPE Cable	31
5.8	Circuit Breaker (Open)	32
5.9	Circuit Breaker (Close)	32
5.10	Disconnecter Switch (Open)	33
5.11	Disconnecter Switch (Close)	33
5.12	Earthing Switch	34
5.13	Current Transformer and Potential Transformer	34
5.14	Bushing	34
5.15	Surge Arrester	35
5.16	Elbow	35
6.1	Single line diagram	38
6.2	Waveform at disconnecter switch	39
6.3	Waveform at bushing	39
6.4	Waveform at transformer	40
6.5	Single line diagram with damping resistor	41
6.6	Waveform at disconnecter switch with damping resistor	42
6.7	Waveform at bushing with damping resistor	42
6.8	Waveform at transformer with damping resistor	43
6.9	Single line diagram with L type compensation	44

6.10	Waveform at disconnecter switch with L type compensation	45
6.11	Waveform at bushing with L type compensation	46
6.12	Waveform at transformer with L type compensation	46
6.13	Single line diagram with T type compensation	48
6.14	Waveform at disconnecter switch with T type compensation	49
6.15	Waveform at bushing with T type compensation	49
6.16	Waveform at transformer with T type compensation	50
6.17	Single line diagram with ferrite ring	51
6.18	Waveform at disconnecter switch with ferrite ring	52
6.19	Waveform at bushing with ferrite ring	52
6.20	Waveform at transformer with ferrite ring	53

List of Tables

- 3.1 VFTO calculation results for the Chinese pilot project 14
- 5.1 Information of components for equivalent circuit [2, 11] 28
- 6.1 Voltage level at different equipment 40
- 6.2 Effect of damping resistor on voltage level 43
- 6.3 Effect of L type hybrid compensation on the VFTO 47
- 6.4 Effect of L type hybrid compensation on the VFTO level 47
- 6.5 Effect of T type hybrid compensation on the VFTO 50
- 6.6 Effect of T type hybrid compensation on the VFTO level 50
- 6.7 Effect of ferrite ring on voltage level 53
- 6.8 Comparison of voltage for all mitigation methods 54
- 6.9 Comparison of voltage level for all mitigation methods 54

Chapter 1

Introduction to Gas Insulated Substation

1.1 Introduction

SF_6 gas insulated substation has been in operation for over 30 years. Consistent technological and design upgrades of the considerable number of components over the span of the time are described by saving in area and volume involved by the substation. In India upto 765 kV gas insulated substations are in service, which catering the urban, industrial and rural areas. SF_6 gas insulated substations are utilized where space limitations, site restrictions or exponential surrounding conditions made it hard to utilize air insulated substations.

GIS units have been working for over 30 years and several units are in service. Almost 80% of the SF_6 gas has been used in GIS units due to its excellent properties [1]. The properties are:

- SF_6 is colourless, odourless and a chemical neutral gas
- SF_6 is 5 times heavier than air, is not toxic and has no dangerous components inside
- SF_6 is nonhazardous gas
- SF_6 has no eco-toxic potential

- SF_6 condensate at low temperature
- SF_6 is a potent greenhouse gas (GWP - $22,800 \times CO_2$)
- SF_6 has excellent electrical characteristics/dielectric properties

GIS technology has some unique features. They are:

- The enclosures have some unique features like light in weight, good conductivity, low eddy-current losses and a high resistance to corrosion.
- GIS can be easily modified with some standard arrangements.



Figure 1.1: Gas Insulated Substation
[13]

The components of gas insulated substation are:

- Circuit Breaker
- Voltage Transformer
- Current Transformer
- Earthing switch
- Disconnecting switch or isolator
- Busbar
- Surge Arrestor
- Enclosures, Conductors, Connectors
- Cable Box
- Gas Density Monitor

1.2 Advantages of GIS

- Compared to conventional substation only 10 % of space require for Gas insulated substation.
- GIS have no risk of fire due to leakage of oil.
- GIS generates no noise and no radio interference.
- GIS offers high level of operational reliability and less maintenance.
- It can be used at urban and industrial area where space is a constraint.
- It can be also used at mountainous area where site preparation, altitude, snow are major problems.
- Overall life cycle cost can be lower than AIS.

1.3 Disdvantages of GIS

- Requires properly pressurized SF_6 gas for electrical insulation of busses, switches, etc. requiring more extensive gas monitoring.
- Initial installed cost of GIS equipment is higher.
- Due to compact design, access for operating and maintenance can be more difficult.
- Particle infusion in GIS.
- Insulating spacers and their reliability.
- SF_6 gas and its reliability.
- Presence of impurities in SF_6 gas.
- Very fast transients in GIS.

For the above mention reasons, in GIS, generated VFTO should be considered as a critical factor to design insulation of GIS components. For the calculation of generated VFTO and waveforms of VFTO , EMTP-RV software is used. To analyze VFTO in gas insulated substation in EMTP-RV software, it is necessary to have an equivalent circuit for each components.

Chapter 2

Literature Review

2.1 Literature Review

Gas Insulated Substations [1] by M.S. Naidu: This book describes about very fast transient over voltage in gas insulation substation. It also describes where VFTO occurs , origin of VFTO, characteristics of VFTO and generation of VFTO.

Analysis of influential factors in determining Very Fast Transient Overvoltages of GIS substations [2] by Babaei, Mehdi, and Ghasem Nourirad: This paper presents the generation of VFTO, components details, modeling of disconnecter switch and calculation of inductance, capacitance, surge impedance, propagation velocity of GIS busbar.

Modeling Guideline For Very Fast Transients in Gas Insulated Substations [3] by J.A. Martinez, P. Chowdhuri, R. Iravani, A. Keri, D. Povh: This paper presents the classification of transients in GIS and the modeling of GIS components.

IEEE Std C37-122 Guide for GIS [4]: This paper describes the rise time and frequency of generated transient waveform.

Transients in Electrical Systems [5] by J.C. Das: This book describes the transient enclosure voltage, operating voltage of GIS, trapped charges and maximum VFTO stresses in gas insulated substation.

Very Fast Transient Overvoltage (VFTO) in Gas Insulated UHV Sub-

station, Cigre 519 [6] and Computation of very fast transient overvoltages in transformer windings [7] by Popov, Marjan: These papers show the general VFTO calculation approach and VFTO suppression using damping resistor.

Estimation of Suppressing very fast transient over voltages in GIS by magnetic rings [8] by Qian Jiali, Guan Yonggang, Zhang Yalin, Xiang Zutao, Liu Weidong, Mitigation of Very Fast Transient Overvoltage in Gas Insulated UHV Substation, Cigre A3-110-2012 [9] and Estimating the size of ferrite for suppressing VFTO in GIS [10] by Lijun, Jin: These papers describe about mitigation of VFTO using ferrite rings in which following topics have been covered:

- General description of ferrite rings
- Location of ferrite rings
- Modeling of ferrite rings

Effective factors on the very fast transient currents and voltage in the GIS [11] by Tavakoli: This paper describes about modeling of GIS components and information of components for equivalent circuit. It also describes the effect of hybrid compensation on VFTO level and effect of compensation resistance on VFTO level.

Modeling guidelines for fast front transients [12] by Imece, Ali F., Daniel W. Durbak, and Hamid Elahi: "This paper describes about modeling of circuit breaker.

Chapter 3

Very Fast Transient Overvoltage

3.1 Where VFTO Occurs?

- VFTO are usually overvoltage with a very steep rate of rise.
- The frequency and amplitude of generated VFTO depends on the layout of the GIS network.
- VFTO voltages at various locations i.e at the disconnecter switch, along the spacer, at the bushing, at the transformer [1].

3.2 Origin of VFTO

- There are two main sources of origin of VFTO in GIS:
 - a. Disconnector switching
 - b. Earth faults
- In both the cases, there is a voltage collapse either between the contacts or between phase and ground, which generates steep voltage surges with very short but finite rise time [1].

3.3 How VFTO generated?

- During the operation of a disconnect switch, restrikes between contacts occur due to the relatively low speed of the moving contact. The inter-contact gap dielectric strength does not recover fast enough compared to the transient recovery voltage that appears across the contacts. Each time transient voltage reaches to dielectric strength across DS contacts, a restrike occurs between contacts and VFTO is generated [2].

3.4 Characteristics of VFTO

- The general shape of a VFTO wave can be a cosine wave with little attenuation. Over this wave are superimposed small high frequency oscillations with large attenuation.
- The time to the first peak ranges from 100 ns to 700 ns. Superimposed high frequency oscillations have magnitudes that are higher than twice the fundamental frequency. The VFTO magnitudes depend on the residual voltage on the DS contacts and the GIS configuration [1].
- A maximum VFTO magnitude has a typical value between 1.5 p.u. and 2.0 p.u. for most GIS configurations. However, values of 2.5 p.u. have been observed in some specific cases [3].

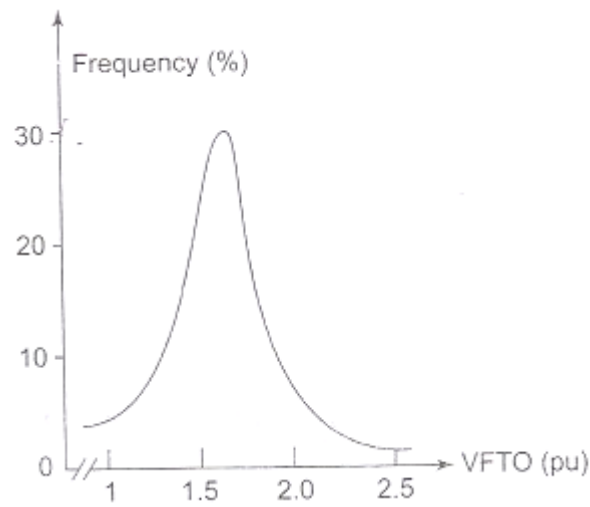


Figure 3.1: Characteristics of VFTO

3.5 Classification of VFTO

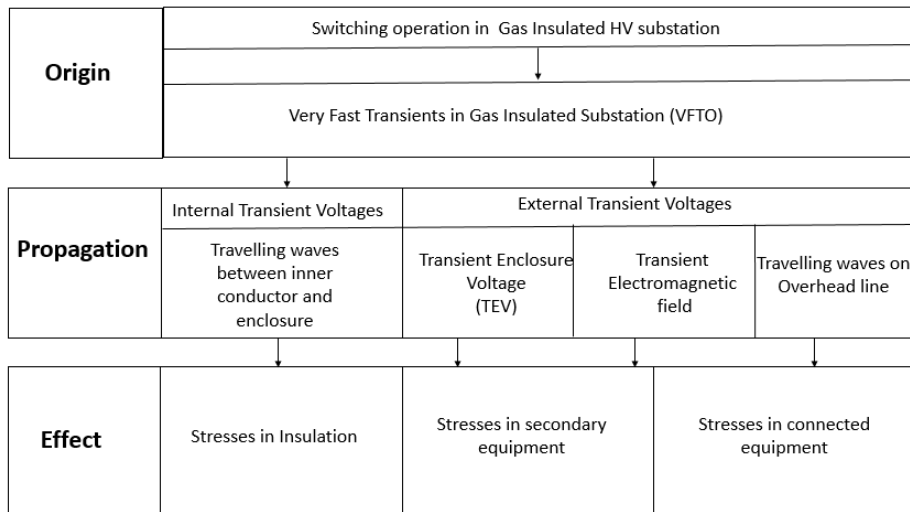


Figure 3.2: Classification of VFTO

3.5.1 Internal transients

- Internal transients produce overvoltage between the inner conductor and traveling waves inside the enclosure. These create insulation stresses in GIS [3].
- Internal transients are generated in GIS during normal operation of disconnector switch. The collapse of voltage across the contacts in 3 to 5 ns and the frequency upto about 100 MHz [4].
- Traveling waves of very short rise time occur which propagate in GIS section. The GIS section can be represented by low-loss distributed parameter transmission line, each section having a certain surge impedance and propagation velocity.

3.5.2 External transients

- These are due to traveling waves and radiation outside the GIS. These include Transient Enclosure Voltage (TEV), Transient Electromagnetic Fields (TEMF), and overvoltages on overhead lines and equipment. These may lead stress on secondary equipment [3].
- Internally generated transients propagate throughout GIS to reach external connections and bushings, where they cause Transient Enclosure Voltage (TEV) and traveling waves that propagate along overhead transmission lines.

Transient Enclosure Voltage

- Transient enclosure voltages are also called Transient Ground Potential Rises (TGPR). These are short-duration high-voltage transients that appear on the enclosure of GIS [5].
- The propagation of an internally generated transient to an air termination and its refraction to outside transmission line/cable [5].

3.6 General VFTO Calculation Approach

Step-1: Calculation of VFTO (Peak Value and Rise time [6])

- System analysis (travelling wave computer simulation program)
- Calculation of the maximum peak value and rise time for the GIS and the connected equipment
- Use of real trapped charge behaviour of the disconnector switch, if known
- The accuracy of the simulation model must be verified.

Step-2: Calculation of the required VFTO withstand voltage for the different equipment by using [6]:

- Co-ordination factor K_c (statistical distribution, inaccuracy of simulation, frequency of occurrence, volume effect)
- Safety factor K_s (atmospheric correction if applicable, aging behaviour in service, quality of installation)
- Test conversion factor K_{tc} (for a given equipment or insulation configuration, the factor to be applied to the required withstand voltage, which describes the different withstand behaviour under VFTO stress compared to the stress with standard LI voltages)

Comparison of calculated required VFTO withstand voltage values with LIWV level

Step-3: Definition of measures according to the insulation co-ordination [6]

- No damping measure required
- Damping measure required

3.6.1 Step1: VFTO Calculation

- The accuracy of a simulation depends on the quality of the model of each individual GIS component. In order to achieve reasonable results even for time

periods of some micro-seconds or for very complex GIS structures, highly accurate models for each internal component and also for external components, connected to the GIS, are necessary.

- An accurate modelling of each individual GIS component makes it possible to reproduce VFTO waveforms. VFTO appearing in GIS are caused not only by DS operation. Other events, such as the operation of a circuit-breaker, the occurrence of a line-to-ground fault or the closing of an earthing switch can also cause VFTO. However, during a DS operation a high number of re-strikes and pre-strikes occur due to the low operating speed of DS compared to a circuit-breaker.

3.6.2 Step2: Required VFTO withstand level - Comparison with LIWV

Case Review

In the GIS, VFTO/Protection Level is more than 1 P.U [Table-3.1]. To damp out this VFTO at GIS, some corrective measures need to be taken.

3.6.3 Step3: Measures according to the insulation co-ordination

- If the required withstand very fast transient overvoltage is equal or lower compared to the insulation withstand strength of the equipment, no damping measures are necessary. If the required withstand VFTO is higher compared to the insulation withstand strength of the equipment, it is necessary to define measures reducing the risk of failures.
- There are two possibilities:
 - a. An increase of the LIWV
 - b. A mitigation of VFTO
- The first choice is easy to realize, but cost-intensive. Nevertheless in some cases this solution has advantages.

Table 3.1: VFTO calculation results for the Chinese pilot project

	Double Busbar
Transformer	
LIWV [kV]	2250
Safety Factor	1.15
Protection Level	1957
VFTO [kV]	942
VFTO [PU]	1.05
VFTO / Protection Level	0.48
GIS	
LIWV [kV]	2400
Safety Factor	1.15
Protection Level	2087
VFTO [kV]	2260
VFTO [PU]	2.52
VFTO / Protection Level	<i>1.08</i>
GIS Bushing	
LIWV [kV]	2400
Safety Factor	1.15
Protection Level	2087
VFTO [kV]	1722
VFTO [PU]	1.92
VFTO / Protection Level	0.83

- The second choice aims for mitigation of amplitudes of VFTO and finally for a suppression of the effect of VFTO on the equipment.

3.7 Operating voltage of GIS

- The operating voltage of GIS can be decided by following way [5]:

For 400 kV GIS,

- System voltage (V_b) = 400 kV
- Surge Impedance of GIS (Z_g) = 84 Ω
- Surge Impedance of transmission line (Z_t) = 315 Ω

The initial amplitude $V_{initial}$ entering GIS can be calculated by,

$$V_{initial} = \frac{V_b Z_g}{Z_g + Z_t + R_s} \quad (3.1)$$

Where R_s is the spark resistance and is neglected initially. This gives 84.21 kV voltage wave entering into GIS.

The value of current wave is given by,

$$I = \frac{V_{initial}}{Z_g} = 1.003kA \quad (3.2)$$

3.8 Trapped Charges

- Due to capacitance, trapped charges might be left on floating section when disconnector switch works on a floating section of substation.
- These trapped charges will reduce gradually, from hours to days, as a result of leakage through spacers. Large trapped charges are undesirable because they will reduce the breakdown strength of insulating surface [5].

3.9 Maximum VFTO stresses

The maximum VFTO stresses occurs due to switching operation of disconnector switch. The maximum voltage is a function of the trapped charge on the load side, the geometry of GIS, and the disconnect voltage at the time of breakdown.

- The trapped charge is mainly dependent on disconnector characteristics. The faster the switch, the greater is the mean value of the voltage.
- For slow switches, the possibility of restrikes and prestrikes in the voltage range of 1.8 to 2 per unit [5].

Chapter 4

Mitigation techniques for VFTO

VFTO mitigation done by following methods.

- VFTO suppression using damping resistor
- VFTO suppression using hybrid compensation
- VFTO suppression using ferrite ring

4.1 VFTO suppression using damping resistor

- During switching operation of disconnector switch, VFTO occurs in GIS. This VFTO may lead to stress on the insulation of GIS components. With the higher voltage levels, the effect of VFTO is significant, so, it is necessary to mitigate this fast transient overvoltages.
- For this, damping resistor method can be used. Damping resistor can be connected in parallel with disconnector switch and a series switch connected with damping resistor. Usually $400\ \Omega$ to $500\ \Omega$ damping resistor will be used to mitigate generated VFTO [7].
- The resistance of the damping resistor could be chosen according to the maximum calculated VFTO and the required mitigation effect. The VFTO decreases with increasing resistance; but the dimension of the disconnector switch increases with increasing resistance [6].

- In addition, special requirements regarding the rate of rise of the voltage across the resistor and the energy absorption must be taken into account.
- So, the selection of damping resistor is one of the major concern.

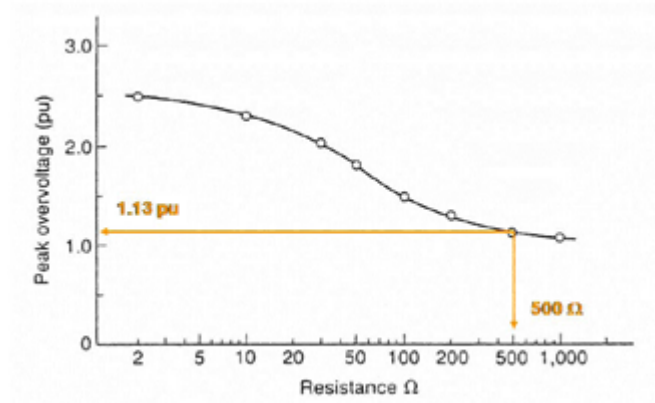


Figure 4.1: VFTO in relation to the resistance of the damping resistor

4.2 VFTO suppression using hybrid compensation

- Combination of series resistor and parallel capacitor can decrease the peak magnitude of VFTO. These series resistor, parallel capacitor are connected in series with disconnector switch.
- L type and T type capacitor-resistor combination is called as hybrid compensation.

4.2.1 L type compensation

- In L type compensation resistor and capacitor connected like L shape.
- So, during switching operation of disconnector switch peak magnitude of VFTO will be reduced.

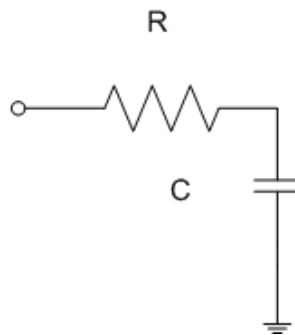


Figure 4.2: L type compensation

4.2.2 T type compensation

- In T type compensation resistor and capacitor connected like T shape.
- So, during switching operation of disconnector switch peak magnitude of VFTO will be reduced.

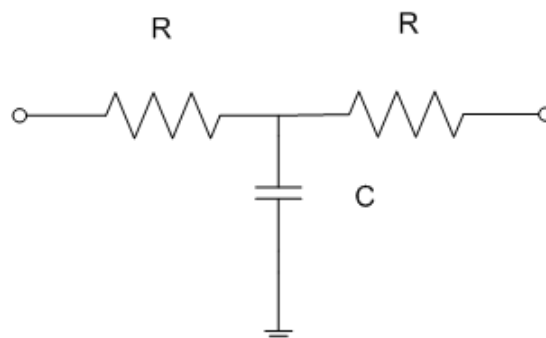


Figure 4.3: T type compensation

4.3 VFTO suppression using ferrite ring

- In this method, high frequency magnetic rings can be used which known as ferrite ring. The suppression of VFTO will be effective by using ferrite ring [8]. The characteristics and design aspects of ferrite rings are discussed in detail.
- The important characteristic of ferrite ring is magnetic saturation and it defines the damping efficiency. In low voltage, magnitude of current is lower. So, the ferrite rings do not saturate, and thus the VFTO mitigation effect is significant for lower voltage simulation [9].
- In higher voltage simulation, current has a higher magnitude. If higher magnitude of current flows through a ferrite ring, the high magnetic field saturates the ferrite material completely. so, the mitigation effect is reduced. The Strength of magnetic field at which the material saturates is increase by layering of ferrite rings [9].
- On the other hand layering the rings with a material of lower permeability also reduces the effective permeability. Therefore, the damping efficiency of the whole ring arrangement decreases. So, to increase the damping efficiency, material which have higher permeability is preferred [9].

Equivalent characteristics of ferrite ring

- The ferrite ring can be connected parallel to disconnector switch to suppress the magnitude of generated VFTO during switching operation of disconnector switch.
- The equivalent circuit for ferrite ring is inductance of the ferrite coil parallel to resistance of the ferrite coil [10].

Design aspects of ferrite ring

- Mn-Zn ferrite is chosen as its high magnetic saturation B_s , $B_s > 470$ mt 25°C. With the of frequency of 100 kHz [10].

Size of ferrite ring

Different ferrite ring can be equivalent to simply form with uniformity magnetic field.

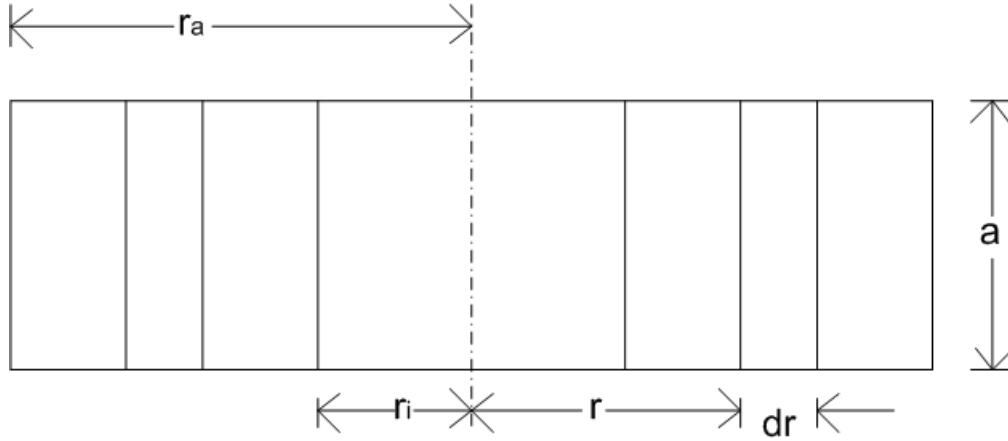


Figure 4.4: Cross section of ferrite ring

It can be similar to a thin ring dr . The size of the ferrite ring is shown as figure (4.4) [10]. Here r_a is outer radius of ferrite ring, r_i is inner radius of ferrite ring and a is height of ferrite ring.

The equivalent inductance L_i is

$$L_i = \mu_0 \mu_i N^2 \frac{A_e}{L_e} \quad (4.1)$$

and

Equivalent resistance R_h is

$$R_h = hf L_i \frac{NI}{L_e} \quad (4.2)$$

where,

μ_i = Relative initial magnetic conductivity

h = Magnetic hysteresis coefficient

N = Number of rings

The ferrite ring is made up of a lot of thin rings dr . So, $NI=2\pi rH$, and area of the section $dA = a.dr$

The differential inductance is

$$dL(r) = \frac{Nd\phi}{I} = N^2 \frac{d\phi}{H2\pi r} = N^2 \frac{Badr}{H2\pi r} \quad (4.3)$$

From $B = \mu_0\mu_i H$

The initial differential inductance is

$$dL_i(r) = \mu_0\mu_i N^2 \frac{a}{2\pi r} \quad (4.4)$$

by adding all the rings, the inductance of the ferrite ring is

$$L_i = \mu_0\mu_i N^2 \frac{a}{2\pi r} \ln \frac{r_a}{r_i} \quad (4.5)$$

$$R_h = hfL_iNI \frac{\frac{1}{r_i} - \frac{1}{r_a}}{\ln \frac{r_a}{r_i}} \quad (4.6)$$

From equation 4.8 and 4.9 we can calculate L_e and A_e

$$L_e = \frac{2\pi \ln \frac{r_a}{r_i}}{\frac{1}{r_i} - \frac{1}{r_a}} \quad (4.7)$$

$$A_e = \frac{a \ln \frac{r_a}{r_i}}{\frac{1}{r_i} - \frac{1}{r_a}} \quad (4.8)$$

Constant magnetic conductivity

- The initial magnetic conductivity (μ_i) for Mn-Zn ferrite ring is between 2000 and 10000. From fig(4.8), $\frac{h}{\mu_i^2}$ varies with frequency while initial magnetic conductivity remains constant.
- The equivalent magnetic field length L_e and section A_e can be calculated from equation (4.9) and (4.10).

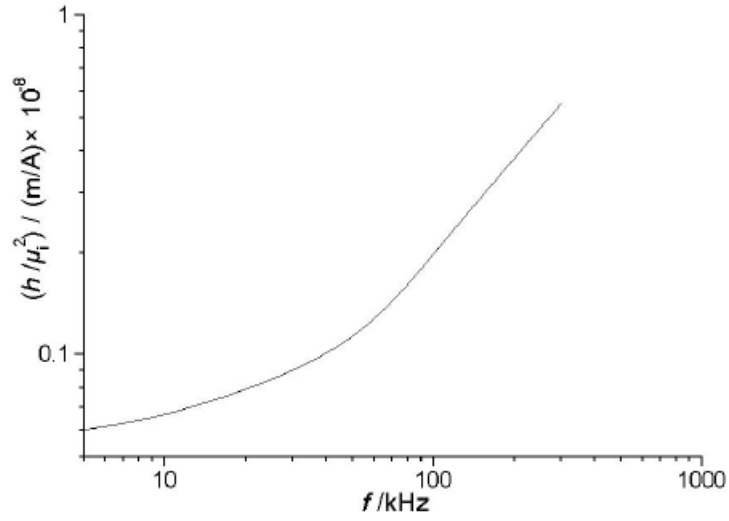


Figure 4.5: frequency and magnetic hysteresis coefficient scale of Mn-Zn ferrite [10]

If the frequency is 100 kHz, magnetic hysteresis coefficient ($\frac{h}{\mu_i^2}$) is 0.18×10^{-8} m/A. For 400 kV GIS, $r_a = 3.5$ mm, $r_i = 1.6$ mm, $a = 1.27$ mm, $I = 1$ kA, $N = 1$, $\mu_i = 4300$.

From equation (4.9) and (4.10),

$$L_e = 7.25 \text{ mm}$$

$$A_e = 1.46 \text{ mm}^2$$

From equation (4.3) and (4.4),

$$L_i = 0.001 \text{ mH}$$

$$R_h = 501.33 \Omega$$

Chapter 5

Calculation and Modeling of GIS Components

5.1 Single Line Diagram of GIS

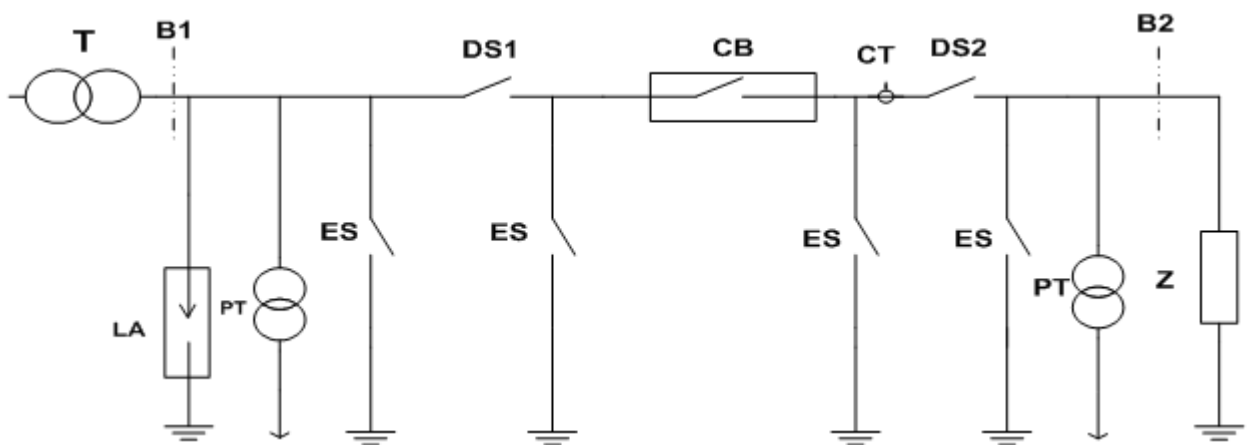


Figure 5.1: Single line Diagram of GIS System

T- Power Transformer, B1- Air to SF_6 Gas Bushing, L.A- Lightning Arrester, P.T- Potential Transformer, E.S- Earthing Switch, D.S- Disconnect Switch, C.B- Circuit Breaker, C.T- Current Transformer, B2- SF_6 gas to XLPE Cable

The typical GIS system consisting of Power Transformer, Air to SF_6 Gas Bushing, Lightning arrester, Potential transformer, Earthing switch, Disconnecter Switch, circuit breaker, Current transformer and SF_6 gas to XLPE (Cross Linked Polyethylene)cable have shown in the single line diagram.

The modeling of GIS makes use of electrical equivalent circuits arrange by lumped elements and distributed parameters. Which is defined by surge impedances and propagation velocity.

The variation of fast transient overvoltages at transformer, bushing and disconnecter switch (DS_1) are calculated during closing operation of disconnecter switch (DS_2) using EMTP-RV.

5.2 Calculation of Various Parameters

5.2.1 Calculation of Transmission Line

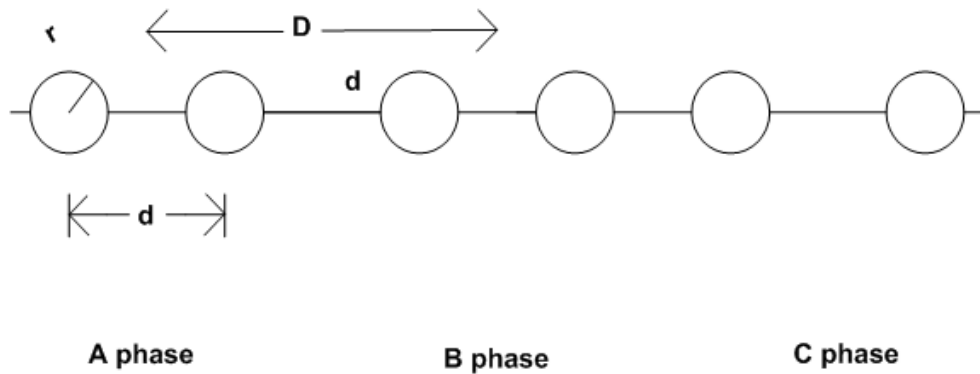


Figure 5.2: Bundle conductor line

- Transmission line can be represented by its equivalent inductance and equivalent capacitance. The following way to determine equivalent inductance and equivalent capacitance:

$$Inductance, L = 2 \times 10^{-7} \ln \frac{GMD}{GMR} \text{ H/m} \quad (5.1)$$

Where,

$$\text{GMD} = \text{Geometrical Mean Distance} = \sqrt[3]{D_{ab}D_{bc}D_{ac}}$$

$$\text{GMR} = \text{Geometrical Mean Radius} = \sqrt{D_s \times d}$$

$$\text{Here } D_s = r e^{-0.25}$$

$$\text{Capacitance, } C = \frac{2\pi\epsilon}{\ln \frac{D_{eq}}{D_s}} \text{ F/m} \quad (5.2)$$

Where,

$$D_{eq} = \sqrt[3]{D_{ab}D_{bc}D_{ac}}$$

$$D_s = \sqrt{r \times d}$$

$$\text{Surge Impedance, } Z = \sqrt{\frac{L}{C}} \Omega \quad (5.3)$$

$$\text{Propagation velocity, } \vartheta = \frac{1}{\sqrt{LC}} \text{ m/s} \quad (5.4)$$

For 400 kV GIS

- Center to center between phase (D) = 12 m
- Distance between sub conductor (d) = 0.45 m
- Radius of each sub conductor (r) = 0.016 m

From above formulas,

L	1.0615 μH
C	0.0107 nF
Z	315 Ω
ϑ	297 m/ μs

5.2.2 Calculation of GIS Busbar

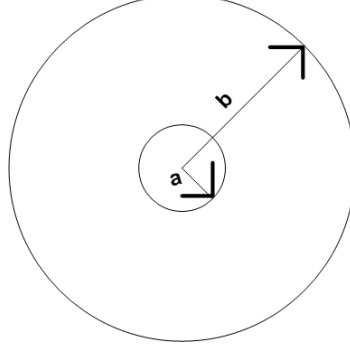


Figure 5.3: Inner conductor and outer enclosure of GIS

- GIS section can be represented by its equivalent inductance and equivalent capacitance. The following way to determine equivalent inductance and equivalent capacitance [2]:

$$\text{Inductance, } L = \mu \ln \frac{b}{a} \quad H \quad (5.5)$$

$$\text{Capacitance, } C = \frac{2\pi\epsilon}{\ln \frac{b}{a}} \quad F \quad (5.6)$$

$$\text{Surge Impedance, } Z = \sqrt{\frac{L}{C}} \quad \Omega \quad (5.7)$$

Where,

μ = magnetic Permeability , $4\pi \times 10^{-7}$ H/m

ϵ = electric Permittivity , 8.854×10^{-12} F/m

b = Inner diameter of GIS enclosure

a = Outer diameter of GIS bus bar

- Propagation velocity in GIS ducts is approximately 0.95 to 0.96 of the speed of light.

For 400 kV GIS,

- a = 12 cm, b = 49.2 cm

From above formulas,

L	0.282 μ H
C	0.039 nF
Z	84 Ω
ϑ	285 m/ μ s

5.2.3 Calculation of XLPE cable

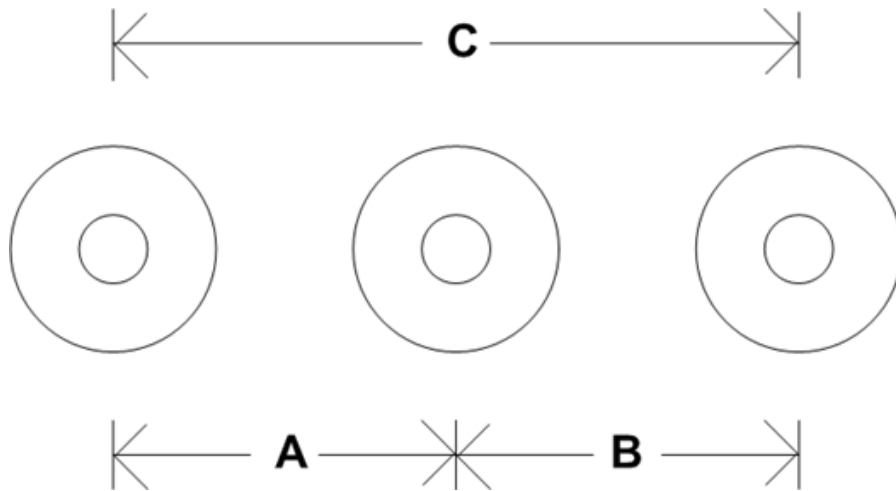


Figure 5.4: Cross section of XLPE cable

- Cable can be represented by its equivalent capacitance and equivalent inductance. The following way to determine equivalent capacitance and equivalent inductance :

$$Inductance, L = \frac{(0.1404 \times \log \frac{\sqrt[3]{A \times B \times C}}{d} + 0.01503) \times K \times L}{10^6} \quad H \quad (5.8)$$

$$Capacitance, C = \frac{7.35 \times SIC \times L}{\log \frac{D}{d} \times 10^6} \quad F \quad (5.9)$$

Where,

D = Cable diameter

d = Conductor diameter

SIC = Dielectric constant

L = Length of cable

K = Installation correction factor

$$\text{Surge Impedance, } Z = \sqrt{\frac{L}{C}} \quad \Omega \quad (5.10)$$

$$\text{Propagation velocity, } \vartheta = \frac{1}{\sqrt{LC}} \quad \text{m/s} \quad (5.11)$$

For 400 kV GIS,

- D = 0.99 inch, d = 0.814 inch, SIC = 2.3 for XLPE cable, L = 460 foot, A,B = 2 inch, C = 4 inch, K = 1.5

From above formulas,

L	0.0797 mH
C	0.03821 μ F
Z	45 Ω
ϑ	165 m/ μ s

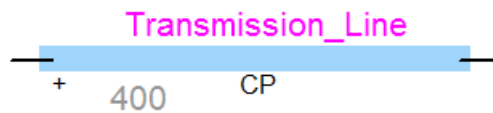
Table 5.1: Information of components for equivalent circuit [2, 11]

Component	Calculated values
Transmission line	Z = 315 Ω , ϑ = 297 m/ μ s
GIS busbar	Z = 85 Ω , ϑ = 285 m/ μ s
XLPE cable	Z = 45 Ω , ϑ = 165 m/ μ s
Potential Transformer (PT)	200 pF capacitance to ground
Current Transformer (CT)	200 pF capacitance to ground
Capacitive Voltage Transformer (CVT)	5 pF capacitance to ground
Eathing Switch	4 pF capacitance to ground
Bushing	Z = 250 Ω & 200 pF capacitance to ground
Surge arrester	15 pF in series with a grounding resistance of 0.1 Ω
Elbow	C= 6 pF capacitance to ground

5.3 Modeling of Various components

5.3.1 Overhead Transmission Line

- Transmission line can be represent by distributed parameters.
- $Z = 315 \Omega$
- $v = 297 \text{ m}/\mu\text{s}$



Constant Parameter (CP) line model (multiphase)

Number of phases

Select model

Distortionless

Continuously transposed

Select type of data

length, R', L', C'

length, R', Z_s, v

length, R', Z_s, τ

Select Units

length any units

R' per unit length

Z_s

v length / s

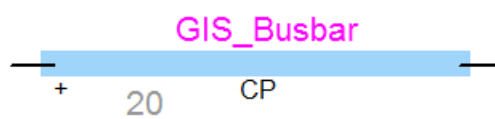
Propagation mode data

MODE	length	R'	Zs	v
0	400	0	315	297E6

Figure 5.5: Transmission Line

5.3.2 GIS Busbar

- GIS busbar can be represent by transmission line with distributed parameters.
- $Z = 84 \Omega$
- $v = 285 \text{ m}/\mu\text{s}$



Constant Parameter (CP) line model (multiphase)

Number of phases ◀ ▶

Select model

Distortionless

Continuously transposed

Select type of data

length, R', L', C'

length, R', Z_s, v

length, R', Z_s, τ

Select Units

length any units

R' per unit length

Z_s

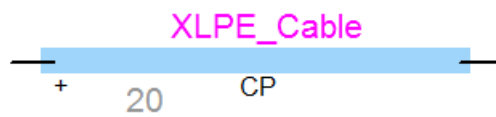
v length / s

Propagation mode data				
MODE	length	R'	Zs	v
0	20	0	84	285E6

Figure 5.6: GIS Busbar

5.3.3 XLPE cable

- XLPE cable can be represent by transmission line with distributed parameters.
- $Z = 85 \Omega$, $v = 165 \text{ m}/\mu\text{s}$



Constant Parameter (CP) line model (multiphase)

Number of phases

Select model
 Distortionless
 Continuously transposed
Select type of data
 length, R', L', C'
 length, R', Z_s, v
 length, R', Z_s, τ

Select Units
 length any units
 R' Ω per unit length
 Z_s Ω
 v length / s

Propagation mode data				
MODE	length	R'	Zs	v
0	20	0	45	165E6

Figure 5.7: XLPE Cable

5.3.4 Circuit Breaker

(a) Circuit Breaker (Open)

- $C_1 = 5 \text{ pF}$
- $C_2 = 10 \text{ pF}$

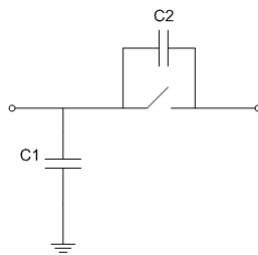


Figure 5.8: Circuit Breaker (Open)

(b) Circuit Breaker (Close)

- Close circuit breaker can be represented by lossless transmission line [2].
- The representation of a closed circuit breaker is complicated because the electrical length is increased and the speed of progression is decreased. [12].
- $C_1 = 5 \text{ pf}$

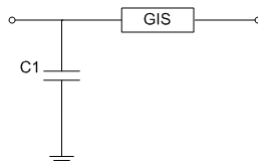


Figure 5.9: Circuit Breaker (Close)

5.3.5 Disconnecter Switch

(a) Disconnecter Switch (Open)

- Open disconnecter switch are modeled as two transmission line in series with a capacitance connected in between them. [2].
- $C_1 = 88 \text{ pF}$, $C_2 = 20 \text{ pF}$
- $Z_1 = 35 \Omega$, $L_1 = 0.5 \text{ m}$

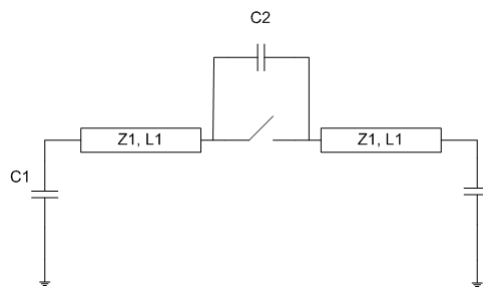


Figure 5.10: Disconnecter Switch (Open)

(b) Disconnecter Switch (Close)

- In close position mention capacitance in open state is replaced by a transmission line with same parameters. [2].

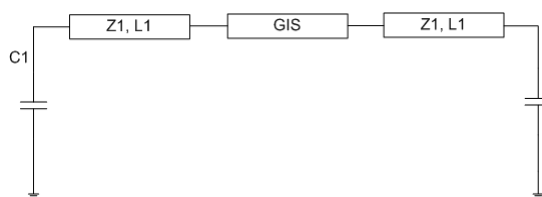


Figure 5.11: Disconnecter Switch (Close)

5.3.6 Earthing Switch

- Lumped capacitance is connected towards ground.
- $C = 4 \text{ pF}$

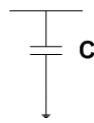


Figure 5.12: Earthing Switch

5.3.7 Current Transformer and Potential Transformer

- Lumped capacitance towards the ground. [2].
- $C = 200 \text{ pF}$

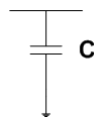


Figure 5.13: Current Transformer and Potential Transformer

5.3.8 Bushing

- Bushing is represented by lossless transmission line with capacitance connected towards ground. [2].
- $Z = 250 \Omega$, $C = 200 \text{ pF}$

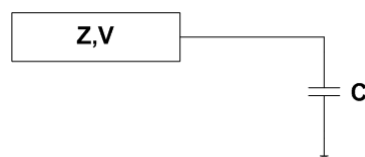


Figure 5.14: Bushing

5.3.9 Surge Arrester

- Capacitance series with resistance to ground. [2].
- $C = 15 \text{ pF}$, $R = 0.1 \Omega$



Figure 5.15: Surge Arrester

5.3.10 Elbow

- Lumped capacitance towards the ground. [2].
- $C = 6 \text{ pF}$

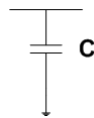


Figure 5.16: Elbow

Chapter 6

Simulation of GIS in EMTP-RV

6.1 Introduction to EMTP-RV

EMTP-RV is a full-featured and technically advanced simulation and analysis professional software for power system transients.

The package is a sophisticated computer program for the simulation of electromagnetic, electromechanical and control systems transients in multiphase electric power systems.

EMTP-RV is utilized worldwide as a reference tool by the main actors of the power system industry. It is suited for a wide variety of power system studies whether they relate to project, design and engineering, or to solving problems and unexplained failures. Its capability to efficiently and quickly perform simulation of huge power systems, its numerical robustness and the stability of the simulation engine contribute to make of EMTP-RV the reference for power systems transients

EMTP-RV's standard library provides a comprehensive and well-documented list of components and function blocks that allow the user to realize easily complete and complex power system studies. It includes:

- Advanced model of electrical machines
- Detailed and precise models of lines and cables
- Complete models of transformers that can model saturation and the hysteresis of the magnetic core

- Extensive library of control devices

6.2 Types of simulation in EMTP-RV

- load flow
- Steady state
- Time-domain
- Frequency scan
- Statistical

6.3 Applications of EMTP-RV

- Network solution
- Short-circuits
- Insulation coordination
- Grid converters
- Power Quality
- Transient Stability
- Renewable energy
- Protection

6.4 Modeling of 400 kV single line diagram

Single line diagram of 400 kV GIS has been modeled in Electromagnet Transient Programme software which is shown in figure (6.1).

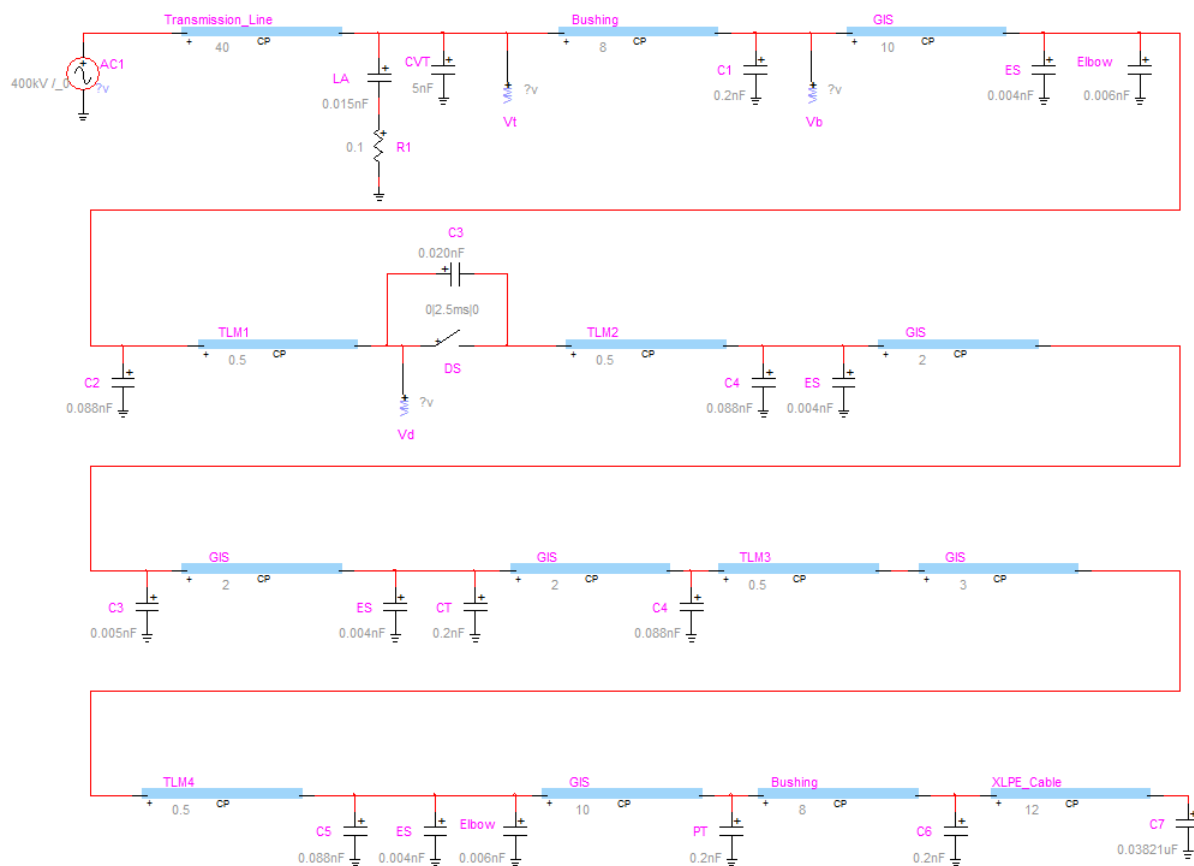


Figure 6.1: Single line diagram

Waveform at Disconnector Switch

Waveform at disconnector switch has been depicted in figure(6.2). It can be seen that transient is there in that waveform because of switching operation of disconnector switch. The peak magnitude of this transient waveform is 1004.58 kV which is too high and further it is required to be reduced.

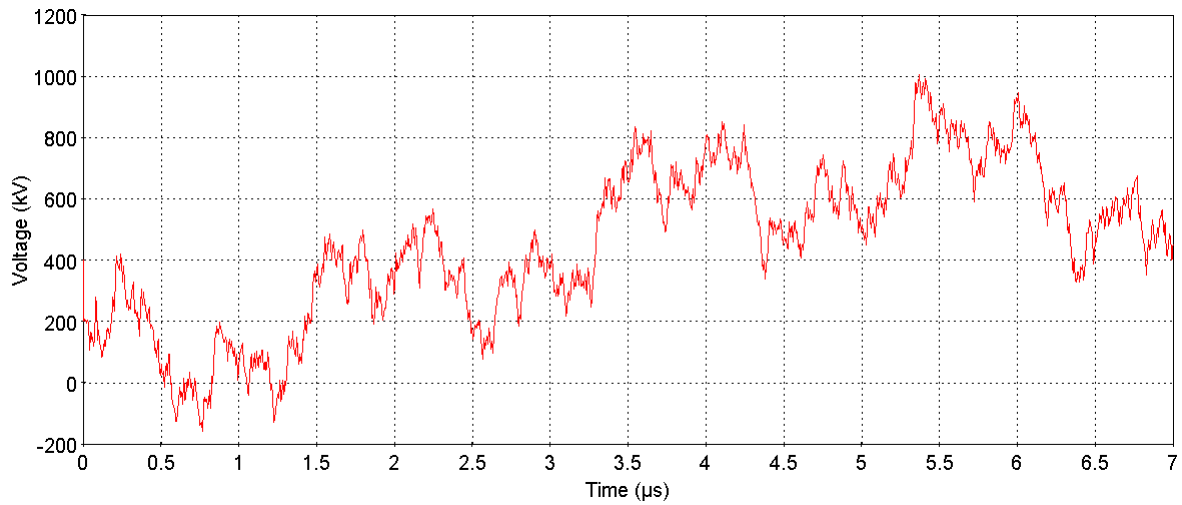


Figure 6.2: Waveform at disconnector switch

Waveform at Bushing

Waveform at bushing has been depicted in figure(6.3). This waveform is due to switching operation of disconnector switch and it is further adversely affected to the bushing and hence at bushing transient has been observed. The peak magnitude of this transient waveform is 1056.14 kV which is too high and further it is required to be reduced.

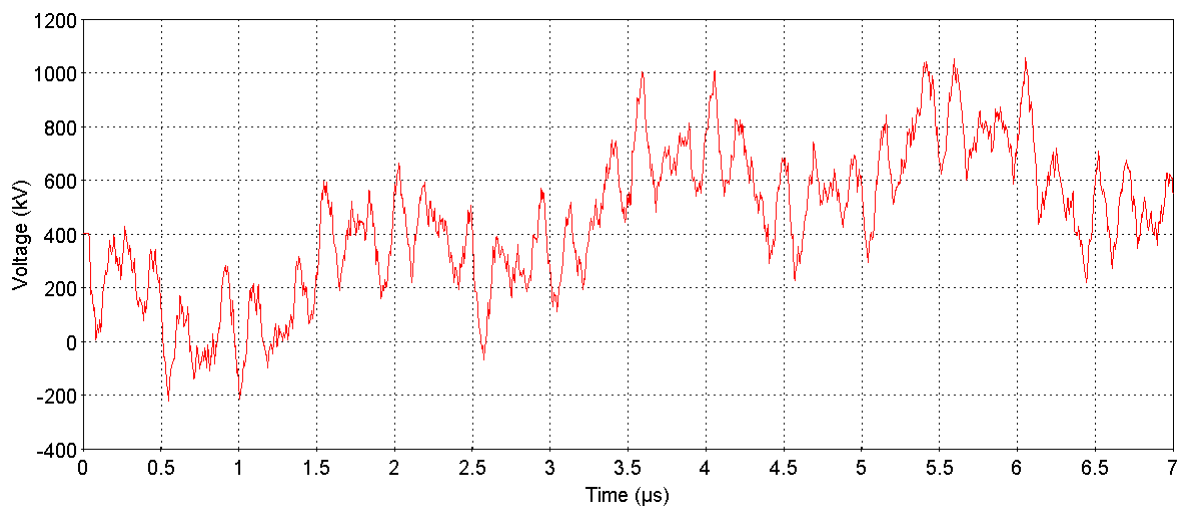


Figure 6.3: Waveform at bushing

Waveform at Transformer

Waveform at transformer has been depicted in figure(6.4). This waveform is due to switching operation of disconnector switch and it is further adversely affected to the transformer magnitude. The peak magnitude of this transient waveform is 893.702 kV which is too high and further it is required to be reduced.

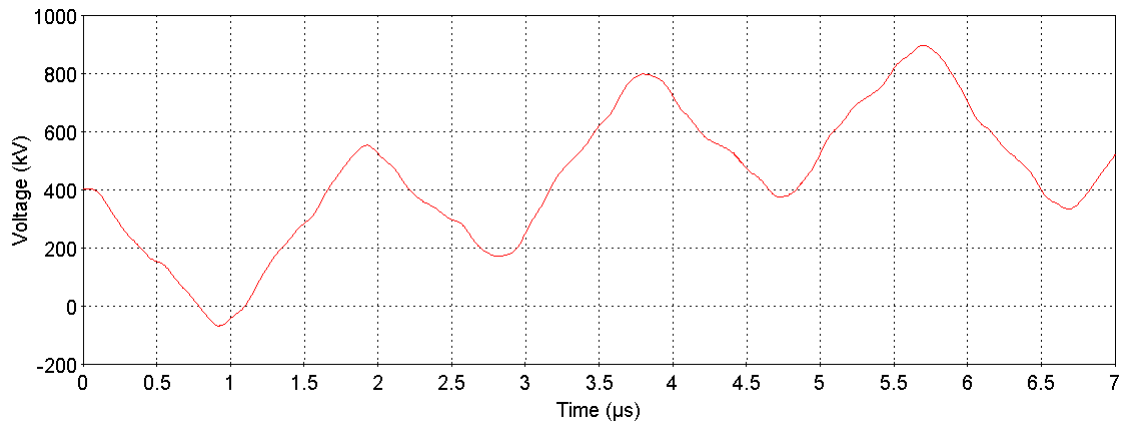


Figure 6.4: Waveform at transformer

Table 6.1: Voltage level at different equipment

Sr. No	Equipment	Measured Voltage (kV)	Rise in Voltage Level
1.	Disconnecter Switch	1004.58	2.51
2.	Bushing	1056.14	2.64
3.	Transformer	893.702	2.23

6.5 Modeling of 400 kV GIS system with Damping Resistor

Single line diagram of 400 kV GIS with damping resistor has been modeled in Electromagnet Transient Programme software which is shown in figure (6.5).

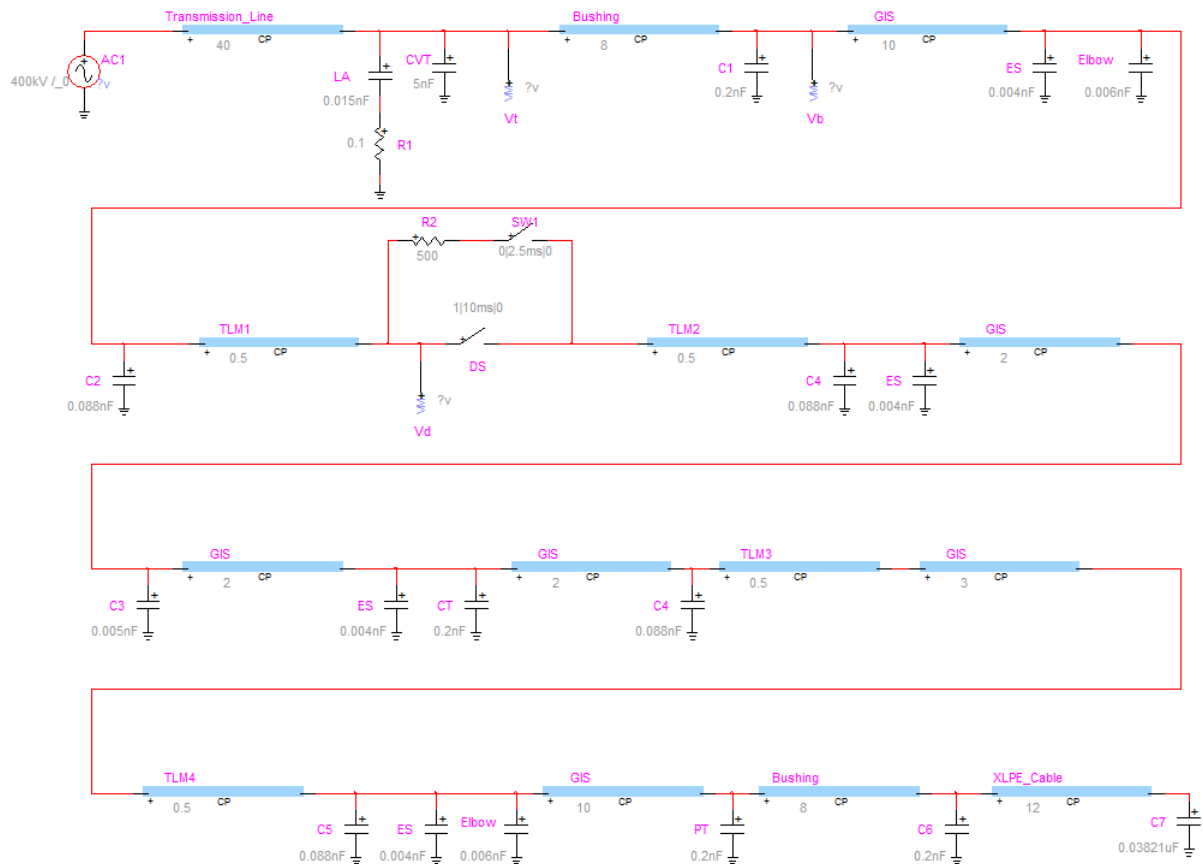


Figure 6.5: Single line diagram with damping resistor

Waveform at Disconnecter Switch

Waveform at disconnecter switch has been depicted in figure(6.6). It can be seen that transient level at initial stage is higher in magnitude but later as time passes ahead it's magnitude is continuously reducing. The peak magnitude of this transient waveform is 452.25 kV which is too much lower compared to magnitude of transient waveform which has been observed at disconnecter switch without using damping resistor.

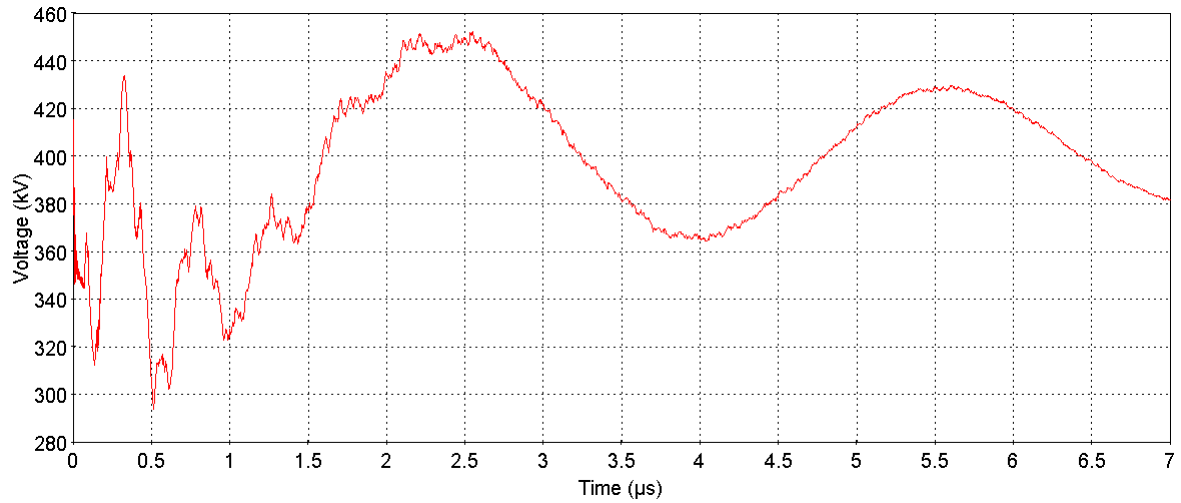


Figure 6.6: Waveform at disconnector switch with damping resistor

Waveform at Bushing

Waveform at bushing has been depicted in figure(6.7). It can be seen that transient level at initial stage is higher in magnitude but later as time passes ahead it's magnitude is continuously reducing. The peak magnitude of this transient waveform is 451.306 kV which is too much lower compared to magnitude of transient waveform which has been observed at bushing without using damping resistor.

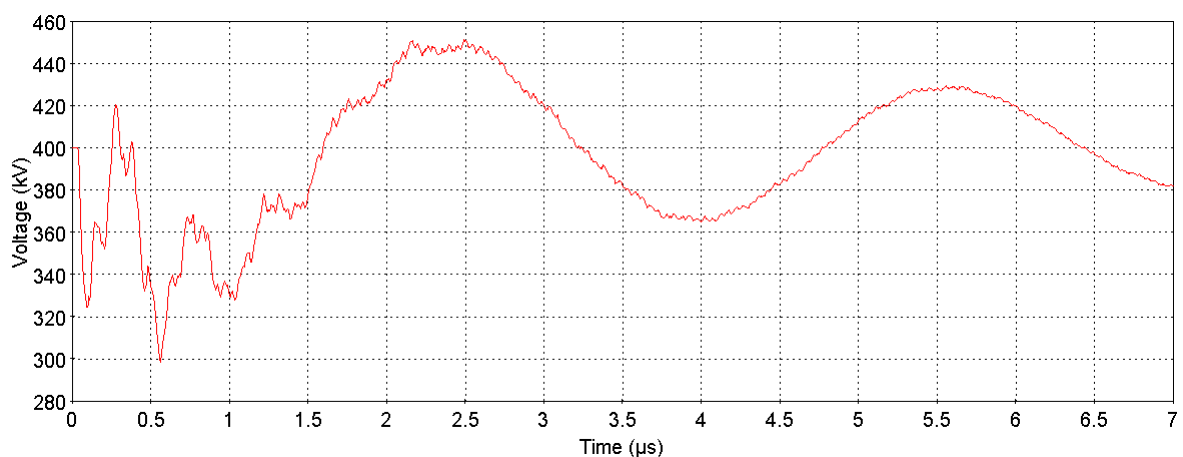


Figure 6.7: Waveform at bushing with damping resistor

Waveform at Transformer

Waveform at transformer has been depicted in figure(6.8). This waveform is due to switching operation of disconnector switch and it is further adversely affected to the transformer magnitude. The peak magnitude of this transient waveform is 448.692 kV which is too much lower compared to magnitude of transient waveform which has been observed at transformer without using damping resistor.

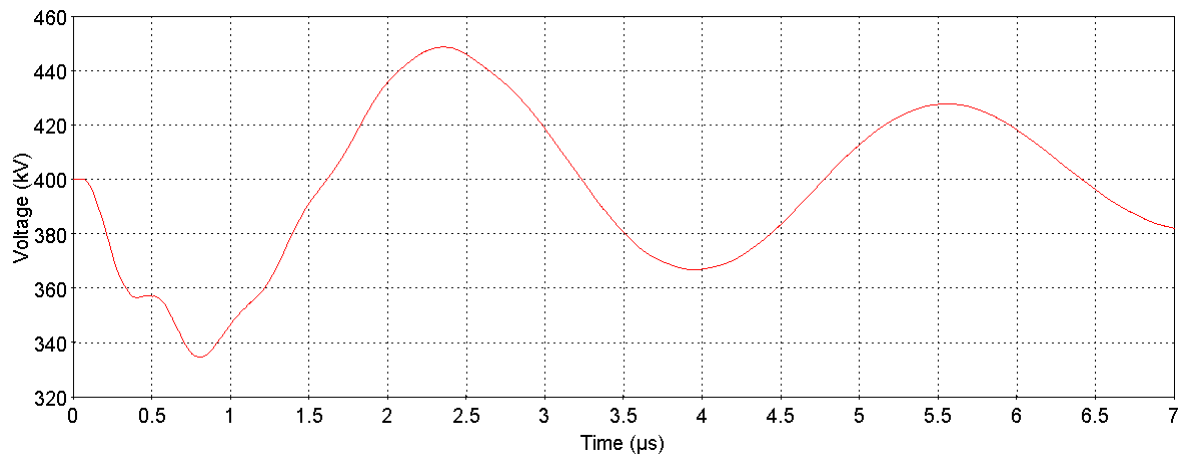


Figure 6.8: Waveform at transformer with damping resistor

Table 6.2: Effect of damping resistor on voltage level

Sr. No	Equipment	Measured Voltage (kV)	Rise in Voltage Level
1.	Disconnecter Switch	452.250	1.121
2.	Bushing	451.306	1.128
3.	Transformer	448.692	1.13

6.6 Effect of hybrid compensation on VFTO

6.6.1 Modeling of 400 kV GIS system with L type compensation

Single line diagram of 400 kV GIS with L type compensation has been modeled in Electromagnet Transient Programme software which is shown in figure (6.9).

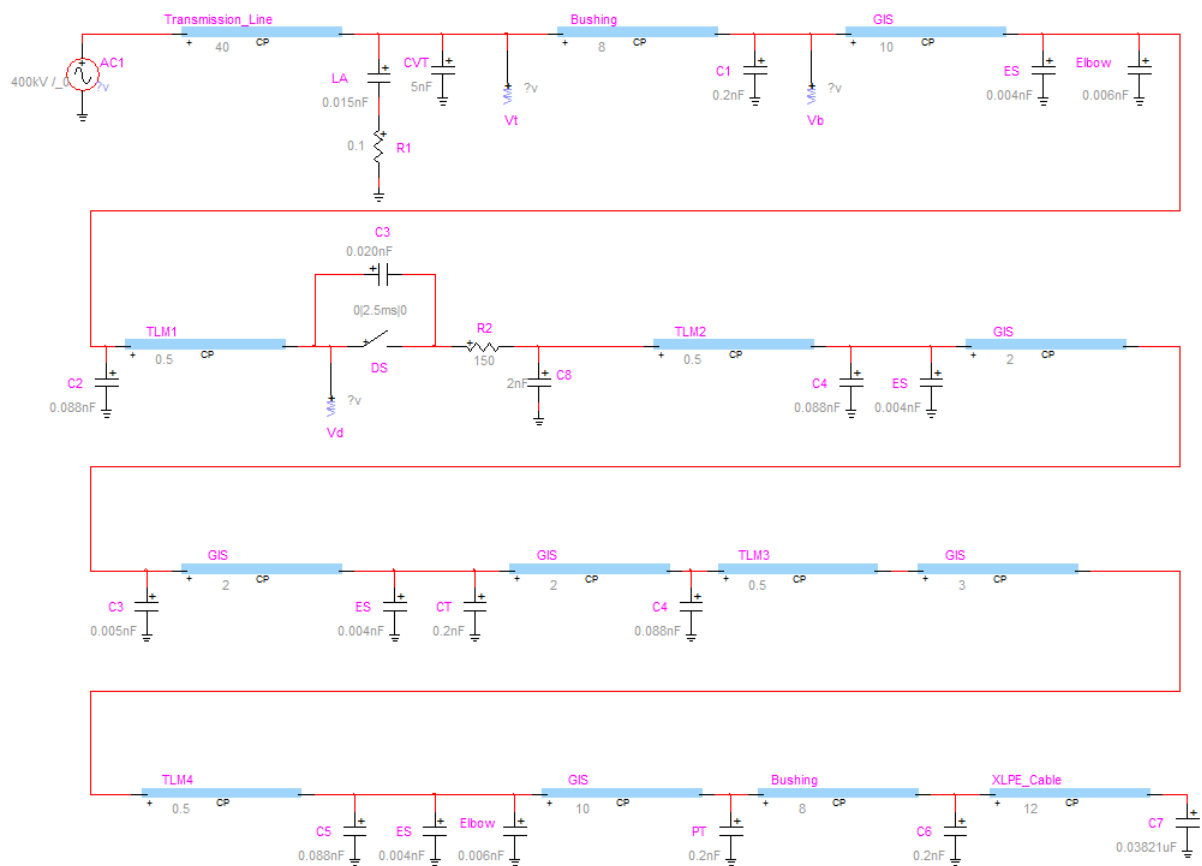


Figure 6.9: Single line diagram with L type compensation

- Table-6.3 shows result of L type compensation with different quantities.
- For example, Combination of $R = 150 \Omega$, $C = 2 \text{ nf}$ will be shown in simulated waveform.

Waveform at Disconnecter Switch

Waveform at disconnector switch has been depicted in figure(6.10). It can be seen that transient level at initial stage is higher in magnitude but later as time passes ahead it's magnitude is continuously reducing. The peak magnitude of this transient waveform is 490.477 kV which is too much lower compared to magnitude of transient waveform which has been observed at disconnector switch without using L type compensation.

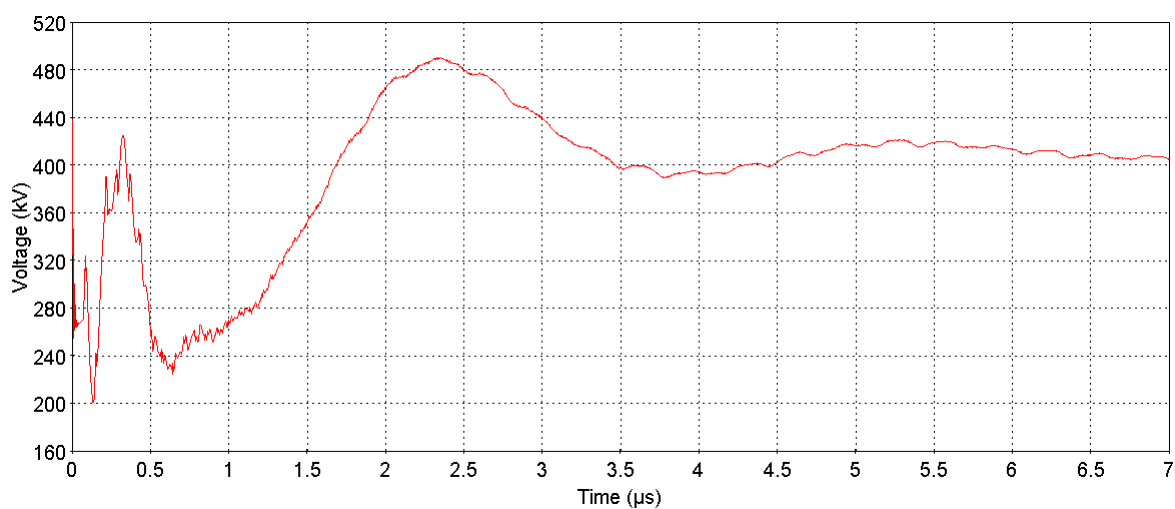


Figure 6.10: Waveform at disconnector switch with L type compensation

Waveform at Bushing

Waveform at bushing has been depicted in figure(6.11). It can be seen that transient level at initial stage is higher in magnitude but later as time passes ahead it's magnitude is continuously reducing. The peak magnitude of this transient waveform is 489.531 kV which is too much lower compared to magnitude of transient waveform which has been observed at bushing without using L type compensation.

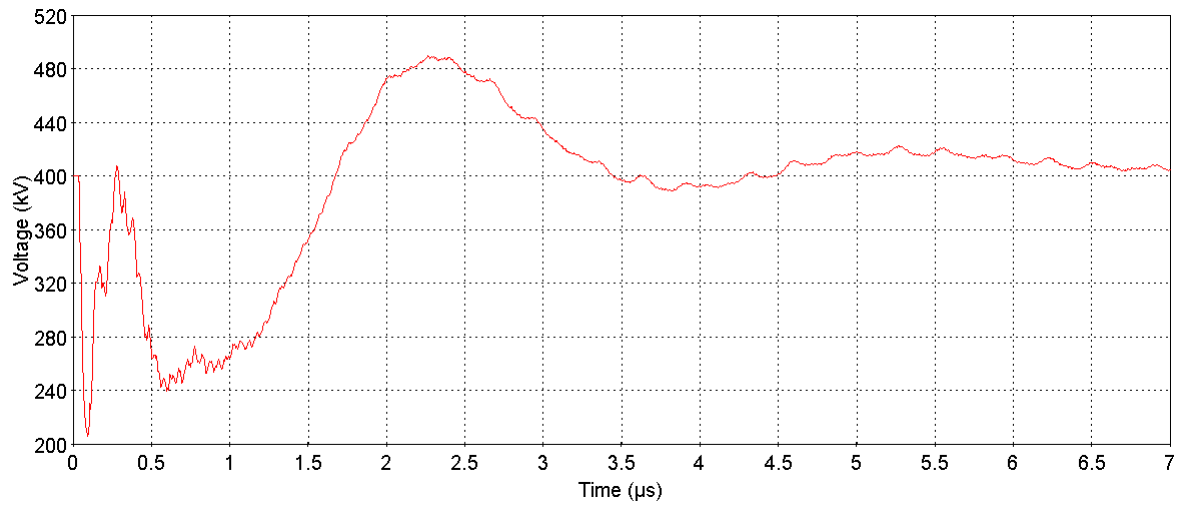


Figure 6.11: Waveform at bushing with L type compensation

Waveform at Transformer

Waveform at transformer has been depicted in figure(6.12). This waveform is due to switching operation of disconnector switch and it is further adversely affected to the transformer magnitude. The peak magnitude of this transient waveform is 488.442 kV which is too much lower compared to magnitude of transient waveform which has been observed at transformer without using L type compensation.

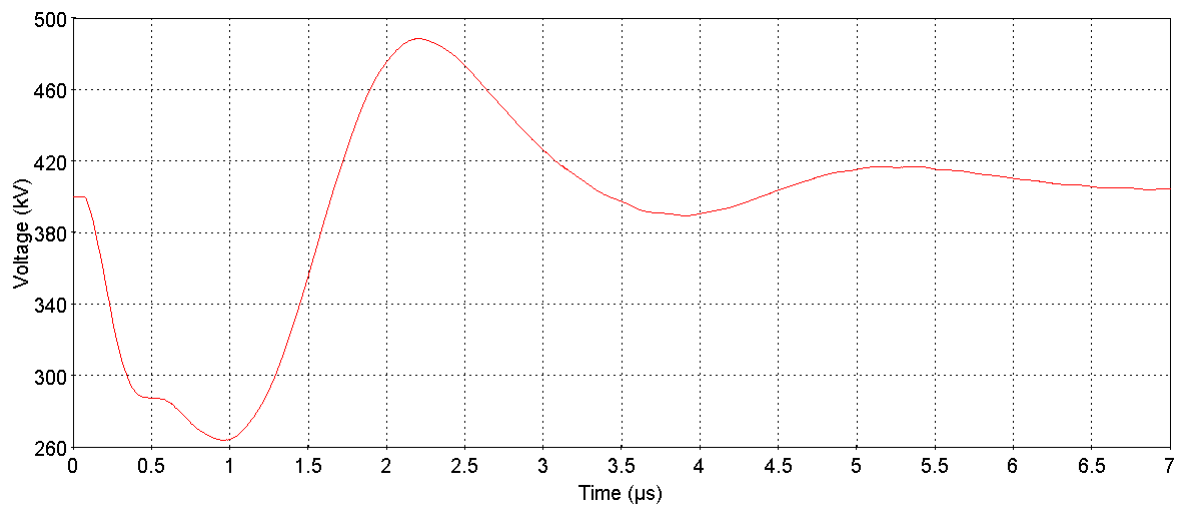


Figure 6.12: Waveform at transformer with L type compensation

Table 6.3: Effect of L type hybrid compensation on the VFTO

Sr. No	L type Compensation	Voltage at disconnecter switch (kV)	Voltage at bushing (kV)	Voltage at transformer (kV)
1.	R = 150 Ω C = 2 nF	490.477	489.531	488.442
2.	R = 100 Ω C = 3 nF	498.567	501.258	504.359

Table 6.4: Effect of L type hybrid compensation on the VFTO level

Sr. No	L type Compensation	Rise in Voltage Level at disconnecter switch	Rise in Voltage Level at bushing	Rise in Voltage Level at transformer
1.	R = 150 Ω C = 2 nF	1.226	1.223	1.221
2.	R = 100 Ω C = 3 nF	1.24	1.25	1.26

6.6.2 Modeling of 400 kV GIS system with T type compensation

Single line diagram of 400 kV GIS with T type compensation has been modeled in Electromagnet Transient Programme software which is shown in figure (6.13).

- Table-6.5 shows result of T type compensation with different quantities.
- For example, Combination of R = 100 Ω , C = 2 nf will be shown in simulated waveform.

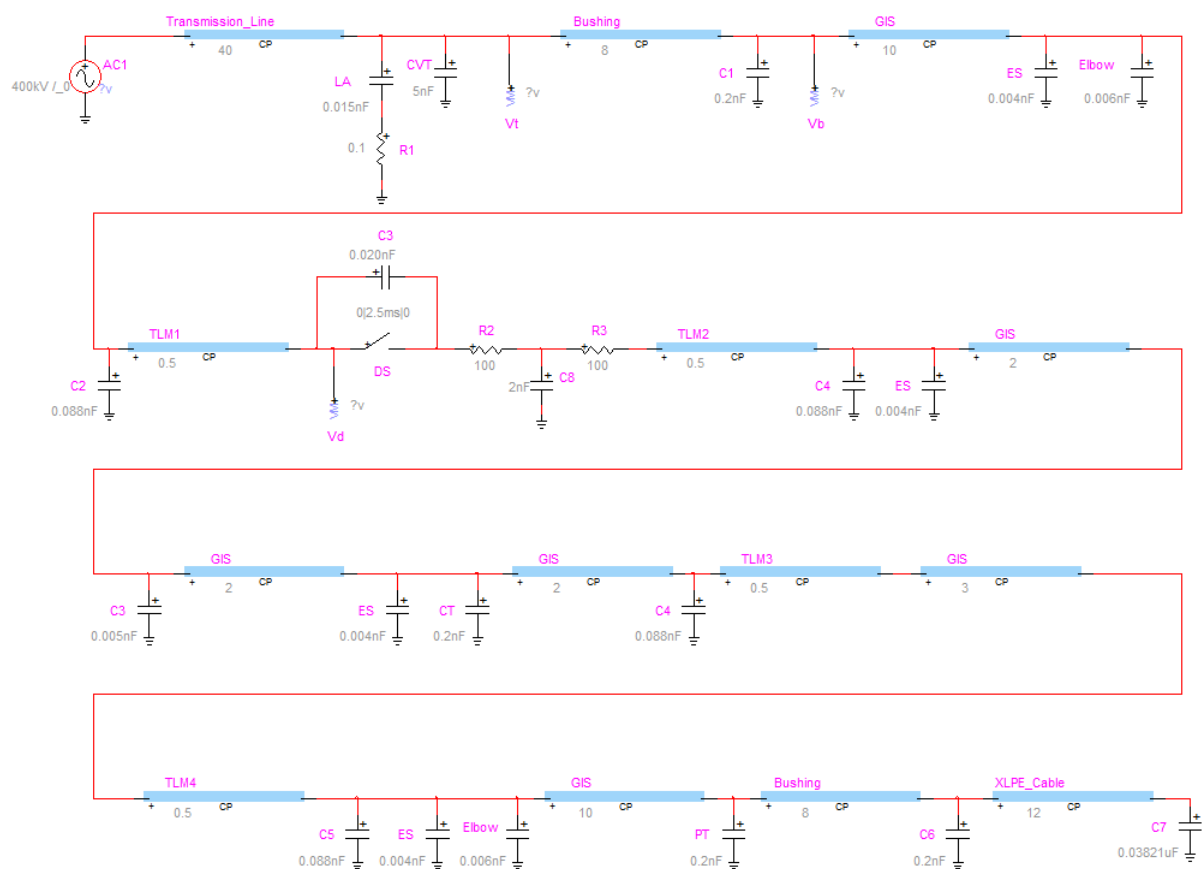


Figure 6.13: Single line diagram with T type compensation

Waveform at Disconnector Switch

Waveform at disconnector switch has been depicted in figure(6.14). It can be seen that transient level at initial stage is higher in magnitude but later as time passes ahead it's magnitude is continuously reducing. The peak magnitude of this transient waveform is 477.110 kV which is too much lower compared to magnitude of transient waveform which has been observed at disconnector switch without using T type compensation.

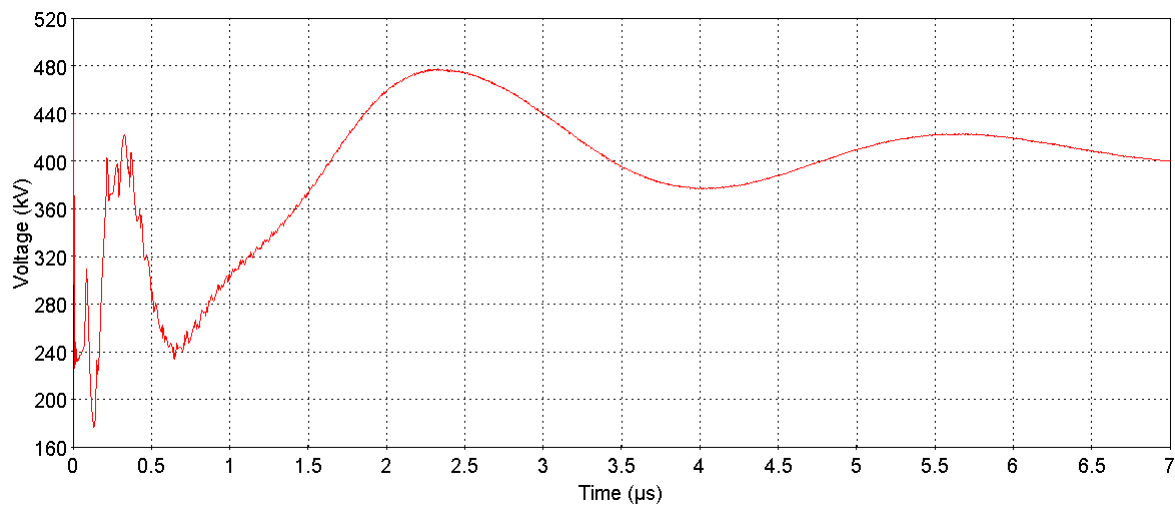


Figure 6.14: Waveform at disconnector switch with T type compensation

Waveform at Bushing

Waveform at bushing has been depicted in figure(6.15). It can be seen that transient level at initial stage is higher in magnitude but later as time passes ahead it's magnitude is continuously reducing. The peak magnitude of this transient waveform is 476.122 kV which is too much lower compared to magnitude of transient waveform which has been observed at bushing without using T type compensation.

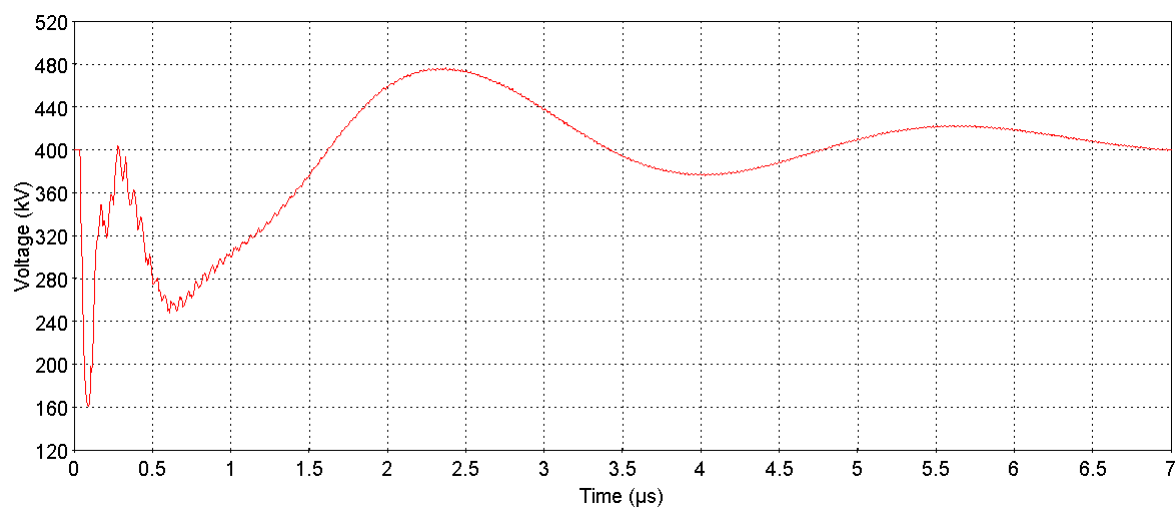


Figure 6.15: Waveform at bushing with T type compensation

Waveform at Transformer

Waveform at transformer has been depicted in figure(6.16). This waveform is due to switching operation of disconnector switch and it is further adversely affected to the transformer magnitude. The peak magnitude of this transient waveform is 471.551 kV which is too much lower compared to magnitude of transient waveform which has been observed at transformer without using T type compensation.

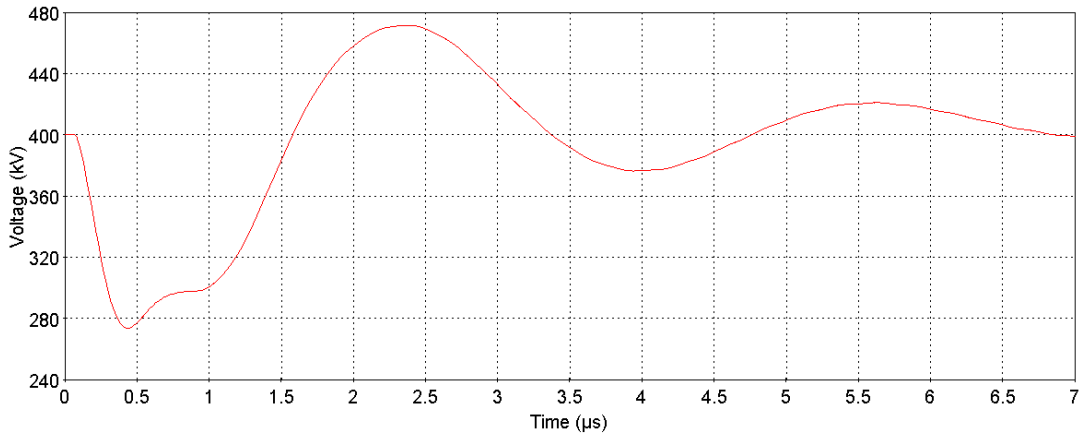


Figure 6.16: Waveform at transformer with T type compensation

Table 6.5: Effect of T type hybrid compensation on the VFTO

Sr. No	T type Compensation	Voltage at disconnector switch (kV)	Voltage at bushing (kV)	Voltage at transformer (kV)
1.	R = 100 Ω C = 2 nF	477.110	476.122	471.551
2.	R = 75 Ω C = 5 nF	482.220	480.745	474.926

Table 6.6: Effect of T type hybrid compensation on the VFTO level

Sr. No	T type Compensation	Rise in Voltage Level at disconnector switch	Rise in Voltage Level at bushing	Rise in Voltage Level at transformer
1.	R = 100 Ω C = 2 nF	1.192	1.190	1.17
2.	R = 75 Ω C = 5 nF	1.205	1.201	1.18

6.7 Modeling of 400 kV GIS System with ferrite ring

Single line diagram of 400 kV GIS with ferrite ring has been modeled in Electromagnet Transient Programme software which is shown in figure (6.17).

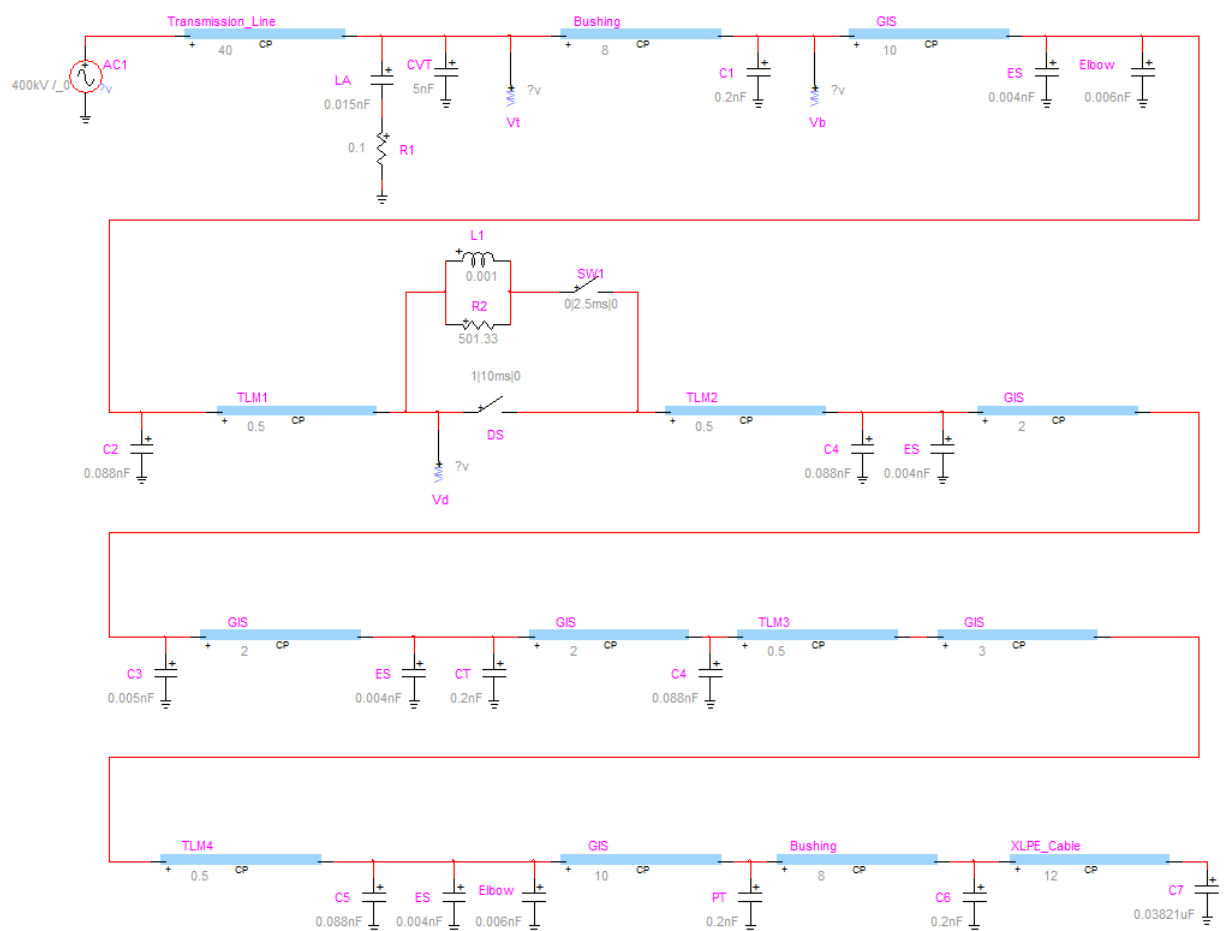


Figure 6.17: Single line diagram with ferrite ring

Waveform at Disconnector Switch

Waveform at disconnector switch has been depicted in figure(6.18). It can be seen that transient level at intial stage is higher in magnitude but later as time passes ahead it's magnitude is continuously reducing. The peak magnitude of this transient waveform is 437.307 kV which is too much lower compared to magnitude of transient waveform which has been observed at disconnector switch without using ferrite ring.

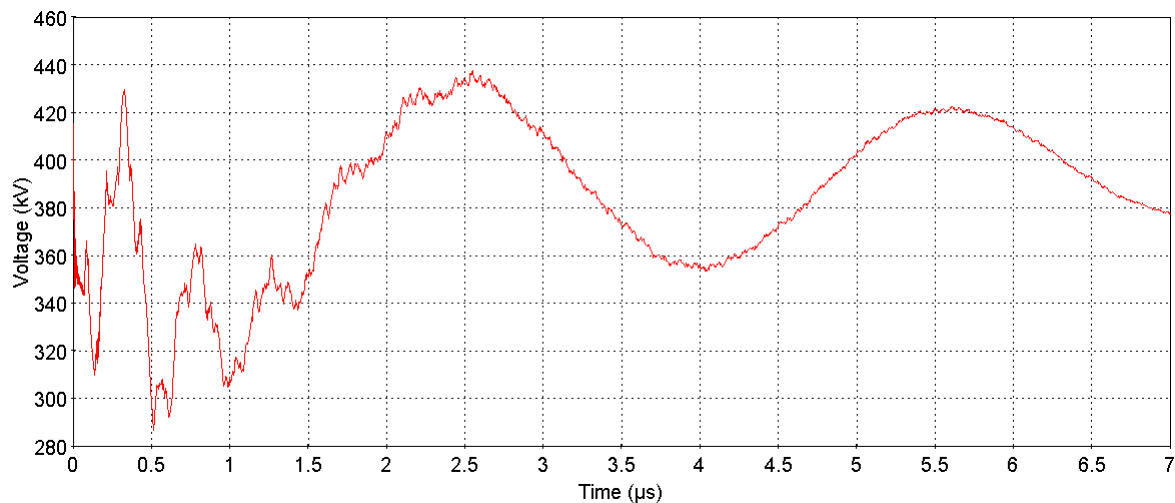


Figure 6.18: Waveform at disconnecter switch with ferrite ring

Waveform at Bushing

Waveform at bushing has been depicted in figure(6.19). It can be seen that transient level at initial stage is higher in magnitude but later as time passes ahead it's magnitude is continuously reducing. The peak magnitude of this transient waveform is 436.559 kV which is too much lower compared to magnitude of transient waveform which has been observed at bushing without using ferrite ring.

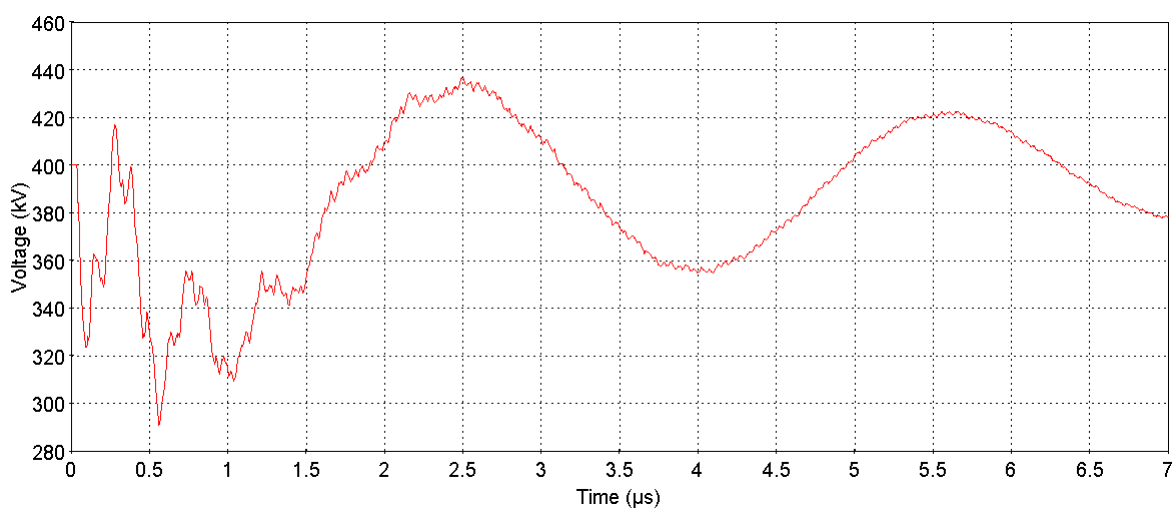


Figure 6.19: Waveform at bushing with ferrite ring

Waveform at Transformer

Waveform at transformer has been depicted in figure(6.20). This waveform is due to switching operation of disconnector switch and it is further adversely affected to the transformer magnitude. The peak magnitude of this transient waveform is 434.425 kV which is too much lower compared to magnitude of transient waveform which has been observed at transformer without using ferrite ring.

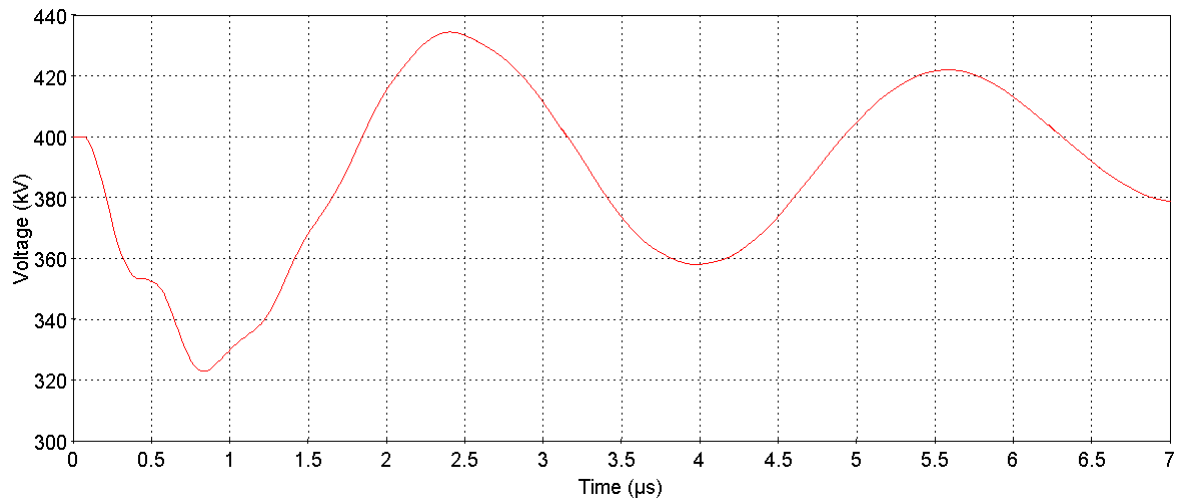


Figure 6.20: Waveform at transformer with ferrite ring

Table 6.7: Effect of ferrite ring on voltage level

Sr. No	Equipment	Measured Voltage (kV)	Rise in Voltage Level
1.	Disconnector Switch	437.307	1.09
2.	Bushing	436.559	1.09
3.	Transformer	434.425	1.08

6.8 Comparison of mitigation methods

Table-6.8 shows comparison of all mitigation techniques. It clearly shows that ferrite ring technique gives best mitigation effect.

Table 6.8: Comparison of voltage for all mitigation methods

Sr. No	Mitigation Methods	Voltage at disconnecter switch (kV)	Voltage at bushing (kV)	Voltage at transformer (kV)
1.	Damping resistor	452.250	451.306	448.692
2.	Ferrite ring	437.307	436.559	434.425
3.	L type compensation	490.477	489.531	488.442
4.	T type compensation	477.110	476.122	471.551

Table 6.9: Comparison of voltage level for all mitigation methods

Sr. No	Mitigation Methods	Rise in Voltage Level at disconnecter switch	Rise in Voltage Level at bushing	Rise in Voltage Level at transformer
1.	Damping resistor	1.13	1.128	1.121
2.	Ferrite ring	1.09	1.09	1.08
3.	L type compensation	1.226	1.223	1.221
4.	T type compensation	1.192	1.190	1.17

Chapter 7

Conclusion and Future scope

7.1 Conclusion

Case-I: GIS modeling

- In case-I 400 kV GIS has been modeled in EMTP-RV software and it has been observed that the magnitude of transient waveform at disconnector switch, at bushing and at transformer due to switching operation of disconnector switch are high in magnitudes and its magnitudes are 1004.58 kV, 1056.14 kV, 893.702 kV respectively. Also its rise in voltage level which is 2.51, 2.64, 2.23 respectively.

Case II: GIS modeling with damping resistor

- In case-II 400 kV GIS has been modeled with damping resistor and it has been observed that the magnitude of transient waveform at disconnector switch, at bushing and at transformer are reduced and reduced magnitude is 451.250 kV, 451.306 kV, 448.692 kV respectively, and it is also observed that there is reduction in its rise in voltage level which is 1.13, 1.128, 1.121 respectively.
- Here it can be seen that with damping resistor transient magnitude and its rise in voltage level have been reduced.

Case III: GIS modeling with hybrid compensation**(a) GIS modeling with L type compensation**

- 400 kV GIS has been modeled with L type compensation and it has been observed that the magnitude of transient waveform at disconnector switch, at bushing and at transformer are reduced and reduced magnitude is 490.477 kV, 489.531 kV, 488.442 kV respectively, and it is also observed that there is reduction in its rise in voltage level which is 1.226, 1.223, 1.221 respectively.
- Here it can be seen that with L type compensation transient magnitude and its rise in voltage level have been reduced.

(b) GIS modeling with T type compensation

- 400 kV GIS has been modeled with T type compensation and it has been observed that the magnitude of transient waveform at disconnector switch, at bushing and at transformer are reduced and reduced magnitude is 477.110 kV, 476.122 kV, 471.551 kV respectively, and it is also observed that there is reduction in its rise in voltage level which is 1.192, 1.190, 1.17 respectively.
- Here it can be seen that with T type compensation transient magnitude and its rise in voltage level have been reduced.

Case IV: GIS modeling with ferrite ring

- In case-IV 400 kV GIS has been modeled with ferrite ring and it has been observed that the magnitude of transient waveform at disconnector switch, at bushing and at transformer are reduced and reduced magnitude is 437.307 kV, 436.559 kV, 434.425 kV respectively, and it is also observed that there is reduction in its rise in voltage level which is 1.09 pu, 1.09 pu, 1.08 pu respectively.
- Here it can be seen that with ferrite ring transient magnitude and its rise in voltage level have been reduced.

- a. After doing simulation of gas insulated substation, it has been observed that VFTO is a major problem in GIS.
- b. Serval methods have been used to mitigate the VFTO out of which ferrite ring method has given best results.

7.2 Future Scope

- Compact design of switchgear by using three phase switchgear in the same enclosure.
- Optimization of GIS design to allow easier maintenance.
- Combination of SF_6 and N_2 gas can improve dielectric strength drastically.
- Development of DC GIS.

References

- [1] M. S. Naidu, Gas Insulated Substations (GIS). IK International Pvt Ltd, 2008.
- [2] Babaei, Mehdi, and Ghasem Nourirad, “Analysis of influential factors in determining Very Fast Transient Overvoltages of GIS substations”, Power Engineering and Optimization Conference (PEOCO), 2014 IEEE 8th International Power Engineering and Optimization Conference (PEOCO2014), 24-25 March 2014.
- [3] J.A. Martinez (Chairman), P. Chowdhuri, R. Iravani, A. Keri, D. Povh, “Modeling Guideline For Very Fast Transients in Gas Insulated Substations”, Report Prepared by the Very Fast Transients Task Force of the IEEE Working Group on Modeling and Analysis of System Transients.
- [4] IEEE Std C37-122 “Guide for GIS”, 1993.
- [5] J.C.Das, Transients in Electrical Systems, McGraw-Hill, 2010.
- [6] Working Group D1.03, “Very Fast Transient Overvoltage (VFTO) in Gas Insulated UHV Substation”, Cigre 519.
- [7] Popov, Marjan, “Computation of very fast transient overvoltages in transformer windings”, Power Delivery, IEEE Transactions on 18.4 (2003): 1268-1274.
- [8] Qian Jiali, Guan Yonggang, Zhang Yalin, Xiang Zutao, Liu Weidong, “Estimation of Suppressing very fast transient over voltages in GIS by magnetic rings”, IEEE 2005.
- [9] Mitigation of Very Fast Transient Overvoltage in Gas Insulated UHV Substation, Cigre A3-110-2012.

- [10] Lijun, Jin, “Estimating the size of ferrite for suppressing VFTO in GIS”, Properties and applications of Dielectric Materials, 2006 IEEE 8th International Conference, 2006.
- [11] A. Tavakoil, A. Gholami, A. Parizad, “Effective factors on the very fast transient currents and voltage in the GIS” Transmission & Distribution Conference & Exposition: IEEE T & D Asia and Pacific, 2009.
- [12] Imece, Ali F., Daniel W. Durbak, and Hamid Elahi, “Modeling guidelines for fast front transients”, IEEE Transactions on Power Delivery 11,CONF-950103–(1996).
- [13] https://www.google.co.in/search?q=Gas+insulated+substation&source=lnms&tbn=isch&sa=X&ved=0ahUKEwjXxp6GncPMAhWBoZQKHQimA9kQ_AUICCGC&biw=1366&bih=657#imgrc=5fkJLQXa7e0F4M%3A